Assessment of the use of differencing satellite imagery as a tool for quantifying landslide impacts from significant storms – a case study in the Uawa catchment, Tolaga Bay

BJ Rosser
S Dellow
S Ashraf

GNS Science Consultancy Report 2019/93
May 2019

GNS SCIENCE
TE PŪ AO

DISCLAIMER

This report has been prepared by the Institute of Geological and Nuclear Sciences Limited (GNS Science) exclusively for and under contract to Gisborne District Council. Unless otherwise agreed in writing by GNS Science, GNS Science accepts no responsibility for any use of or reliance on any contents of this report by any person other than Gisborne District Council and shall not be liable to any person other than Gisborne District Council, on any ground, for any loss, damage or expense arising from such use or reliance.

Use of Data:

Date that GNS Science can use associated data: April 2019

BIBLIOGRAPHIC REFERENCE

Rosser BJ; Ashraf S; Dellow S. 2019. Assessment of the use of differencing satellite imagery as a tool for quantifying landslide impacts from significant storms – a case study in the Uawa catchment, Tolaga Bay. Lower Hutt (NZ): GNS Science. 51 p. Consultancy Report 2019/93.

CONTENTS

EXECUTIVE SUMMARY ..... **V**

1.0 INTRODUCTION **1**

1.1 Purpose of The Report 1
1.2 Data Sources 2

2.0 JUNE 2018 STORM EVENTS **3**

2.1 3rd to 4th June 2018 3
2.2 11th to 12th June 2018 6

3.0 STUDY AREA **7**

3.1 Geology and Geomorphology 7
3.2 Erosion Terrains 8
3.3 Land Cover 8

4.0 LANDSLIDE RECONNAISSANCE **16**

4.1 Landslide Types and Examples 16
4.2 Downstream Deposition and Impacts 16

5.0 ASSESSMENT OF SATELLITE IMAGERY FOR LANDSLIDE MAPPING **27**

5.1 Data Sources 27
5.1.1 Sentinel imagery 27
5.1.2 Planet Dove imagery 28
5.1.3 Planet SkySat imagery 28
5.2 Mapping Methodology 29
5.2.1 Landslides 29
5.2.2 Overbank deposition 30
5.2.3 Assessment of satellite differencing accuracy 31

6.0 ANALYSIS OF SEDIMENT LOSSES AND GAINS **36**

6.1 Scaling from Landslide Area to Volumes 36
6.2 Scaling Automated Mapping to Manual Mapping 36
6.3 Sediment Delivery 38
6.4 Sediment Deposition 42

7.0 LANDSLIDE SEVERITY AND DISTRIBUTION **43**

7.1 Controls on Landslide Distribution 43
7.1.1 Rainfall 43
7.1.2 Geology/Erosion terrain 44
7.1.3 Slope 44
7.1.4 Aspect 45
7.1.5 Vegetation 46

8.0 DISCUSSION **47**

8.1 Landslides Triggered by the Queen's Birthday Storm 47
8.2 Limitations of Satellite Imagery Differencing to Detect Landslides 48

9.0 CONCLUSIONS 49

10.0 ACKNOWLEDGEMENTS 50

11.0 REFERENCES 50

FIGURES

Figure 2.1 Contoured rain gauge data from GDC showing the 8-hour maximum rainfall 4

Figure 2.2 12-hour rain radar data from MetService. 5

Figure 3.1 Simplified geology of the Uawa catchment (from Mazengarb and Speden, 2000). 10

Figure 3.2 Landforms in the Uawa catchment. 11

Figure 3.3 Distribution of erosion terrains in the Uawa catchment. 12

Figure 3.4 Distribution of land cover classes in the Uawa catchment from the LCDBv4.1 14

Figure 4.1 Extensive shallow soil slides, debris slides and debris flows, on newly harvested areas in the headwaters of the Mangatoitoi 17

Figure 4.2 Extensive shallow soil slides, debris slides and debris flows in a newly forested area in the Mangatoitoi stream tributary of the Mangaheia River 17

Figure 4.3 Extensive shallow soil slides, debris slides and debris flows in a newly forested area in the upper Takamapohia Stream, Te Mauranga Forest, Mangatokerau catchment 18

Figure 4.4 Debris slides and debris flows in established maturing forests in the headwaters of the Waiau River 18

Figure 4.5 Debris flows initiated in established pine plantations in the headwaters of the Mangatokerau River 19

Figure 4.6 Skid haul operation in a newly harvested area in the head of Tapaue Stream, Paroa Forest, Uawa catchment. 19

Figure 4.7 Shallow soil slides and debris flows with source areas in fill slopes below a landing on recently logged slopes in the headwaters of Takamapohia Stream, tributary of the Mangatokerau River 20

Figure 4.8 Soil slides and debris flows with source areas in fill used to construct a landing in the Mangatoitoi Stream, Mangaheia catchment near Five Bridges (Uawa Forest) 20

Figure 4.9 Debris flow initiated in the fill slope of a forestry road in the head of Mangatoitoi Stream, Mangaheia catchment near Five Bridges (Uawa Forest) 21

Figure 4.10 Soil and rock falls, soil and rock slides, and soil flows originating on or above cut slopes above Tirohanga forestry road between Kaimonona and Te Kokokakahi Streams in the headwaters of Mangatokerau River 21

Figure 4.11 Largely unaffected pasture on hilly steep lands developed on cohesive, generally weak to moderately strong Tertiary-aged rocks in the headwaters of the Waiau River west of Fernside Road 22

Figure 4.12 Large rotational slump in the headwaters of Waiau River east of Fernside Road 22

Figure 4.13 Debris slide directly coupled to the channel of the Mangaheia River, on Drysdale forestry road above Five Bridges. Sediment and woody debris have been delivered directly to the channel. 23

Figure 4.14 Woody debris generated from logging activities and transported by shallow soil slides, debris slides and debris flows stored in first order stream channels in the headwaters of Tapaue Stream, Paroa Forest, Uawa Catchment. 23

Figure 4.15 Bank erosion in the middle reaches of the Mangaheia River, downstream of Takapau Road/Wigan Bridge 24

Figure 4.16 Woody debris deposited on the floodplain of the Mangatokerau River upstream of the Paroa Road Bridge showing Mangatokerau Road 24
Figure 4.17 Woody debris deposited on the floodplain of the Mangatokerau River downstream from Mangatokerau Road 25
Figure 4.18 Sediment and woody debris deposited on the Tapaue Stream floodplain on Paroa Station 25
Figure 4.19 Sediment and woody debris deposited on the Tapaue Stream floodplain, Paroa Road 26
Figure 4.20 Sediment deposition on the floodplain of the Mangaheia River at Wigan Bridge 26
Figure 5.1 Extents of available post-storm satellite imagery: a) Sentinel, b) Planet Dove and c) Planet SkySat. 27
Figure 5.2 Mapped landslides from the Queen's Birthday storm 30
Figure 5.3 Mapped areas of overbank deposition from differencing of NDWI derived from Sentinel imagery. 31
Figure 5.4 Landslide mapping in selected 1 km^2 areas using automated differencing for Sentinel and Planet Dove imagery and manual mapping of Planet SkySat images. 32
Figure 5.5 Comparison of landslides mapped on pasture 33
a) manually on 0.8 m resolution SkySat imagery, to automatic classification of landslides from b) 3m resolution Planet and c) 10 m resolution Sentinel imagery. 33
Figure 5.6 Comparison of landslides mapped on forestry 33
Figure 5.7 Comparison of landslides mapped on logged areas 33
Figure 5.8 Comparison of areas of overbank deposition generated by the NDWI 35
Figure 6.1 Area to volume scaling relationships for landslides in the Waipaoa catchment triggered by Cyclone Bola 37
Figure 7.1 Mapped landslide distribution from the Queen's Birthday storm in the Uawa catchment using automatic extraction of landslides from a) Sentinel and b) Dove imagery differencing. 43
Figure 7.2 Relationship between rainfall (8hr) and landslide density. 44
Figure 7.3 Relationship between slope and landslide density. 45
Figure 7.4 Slope aspect of hillslopes that landslides were triggered on compared to the aspect of hillslopes in the Uawa catchment 45

TABLES

Table 2.1 Rainfall data for the June 2018 rainstorms in the Uawa and Pakarae catchments (Data from GDC). 3
Table 3.1 Statistical data for geological units in the Uawa catchment based on the mapping of Mazengarb and Speden (2000). 7
Table 3.2 Relationship between Waipaoa erosion terrains 9
Table 3.3 Erosion terrain descriptions for the Uawa catchment. 13
Table 3.4 Land cover vegetation classes in the Uawa catchment 15
Table 5.1 Comparison of areas, resolution and mapping methods used for each type of Satellite imagery. 27
Table 5.2 Sentinel datasets used to for differencing 28
Table 5.3 Images acquired from Planet's Dove satellite constellation for this analysis. 28
Table 5.4 Images acquired from Planet SkySat satellites. 28
Table 5.5 Comparison of automated landslide recognition results from differencing pre- and post-event Sentinel and Planet Dove satellite images. 31

Table 5.6 Comparison of landslide statistics obtained from the different Satellite images 34
Table 6.1 Landslide size distribution for the three main erosion terrains in the Uawa catchment 38
Table 6.2 Landslide statistics (number, percentage and landslide density) for the June 2018 rainstorms in the Uawa catchment for each vegetation class. 39
Table 6.3 Numbers of landslides from Dove and Sentinel automated differencing results.....40
Table 6.4 Automated differencing of Sentinel imagery scaled to manual mapping to produce numbers relative to the size distribution and volumes of sediment per erosion terrain.....41
Table 6.5 Areas of deposition in the Queen's Birthday Storm as recorded by Sentinel and Dove satellites. 42
Table 7.1 Numbers of landslides and density using the numbers of landslides generated from Sentinel imagery differencing. 44
Table 7.2 Landslide numbers (scaled to manual mapping) and densities for the main vegetation classes in the Uawa catchment.....46

EXECUTIVE SUMMARY

On 3rd and 4th June 2018, torrential rain in the area inland from Tolaga Bay, Gisborne Region, triggered thousands of landslides. The headwaters of the Uawa catchment received 234 mm of rain in 24 hours with most falling over an eight-hour period. Many of the landslides were in newly harvested areas in commercial forests and carried woody debris left on hillsides after harvest, down into the rivers and streams. Sixty-one bridges in the Uawa catchment were closed due to flooding and the build-up of woody debris against the bridges. Farms in the Mangatokerau and Tauwhareparae Valleys sustained substantial damage. GDC estimated the storm cost the District more than $10M.

On 11th to 12th June 2018, a further 270 mm of rain fell in 48 hours north of Gisborne (Uawa and Mata catchments) resulted in some new land sliding and reactivation and remobilization of landslides and landslide debris from the previous storm. While peak rainfall intensities were lower than the first storm, the duration of intense rainfall was longer and the distribution more widespread (Cave 2018a).

There were approximately 6680 landslides triggered by the June 2018 rainstorms in the Uawa catchment. They occurred over an area of about 415 km^2, on the western and northern parts of the catchment. The average landslide density was 16.1 landslide/km^2 and the total area of landslides was approximately 2.4 km^2 (from Planet differencing).

The estimated volume of sediment produced by landslides in the storm event was 4,200,000 m^3, approximately half of which (2.1 M m^3 or 2.6 M tonnes) was delivered to the Uawa River system. An area of 426 ha was affected by overbank sedimentation during the flooding associated with the storm event. The estimated average depth of overbank sediment ranged from 25 to 50 mm, giving a total of volume of roughly 100,000 to 200,000 m^3.

Landslide densities were highest in areas of exotic plantation forest that had been logged within the last 3 years. Landslide densities were also relatively high on areas that had been logged 3-6 years ago and in areas of established exotic forest. Landslide densities were much lower on areas of pasture. In the recently logged areas, about half (46%) of the landslides were associated with forestry infrastructure such as logging roads and haul sites or landings. The percentage of landslides that were associated with forestry infrastructure on slopes in established exotic forest was also relatively high (30%).

Although differencing of satellite imagery is quicker and cheaper than traditional landslide mapping methods, the errors and misclassifications are potentially significant, and to achieve a landslide distribution and statistics that accurately portrays the landslides on the ground requires considerable checking and editing of landslide polygons. At the minimum, a comparison of landslide distributions obtained by satellite images should be checked against what would be produced by manual mapping using high resolution satellite imagery or aerial photography, so that appropriate scaling relationships can be developed for different vegetation types.

This page left intentionally blank

1.0 INTRODUCTION

On 3rd and 4thJune 2018, torrential rain in the area inland from Tolaga Bay, Gisborne Region, triggered many landslides. The headwaters of the Uawa catchment received 234 mm of rain in 24 hours with most of the rain falling over an eight-hour period from about midnight on June 3rd to 8.30am on June 4th. The rainfall triggered thousands of landslides and debris flows. Many of the landslides were in newly harvested areas in commercial forests and carried woody debris left on hillsides after harvest, down into the rivers and streams. Sixty-one bridges in the Uawa catchment were closed due to flooding and the build-up of woody debris against the bridges. Farms in the Mangatokerau and Tauwhareparae Valleys sustained substantial damage. Gisborne District Council (GDC) estimated the storm cost the District more than $10M.

The flood associated with the first Queen's Birthday event resulted in around 47,000 m^3 of woody debris being deposited on the beach at Tolaga Bay and at least a further 400,000 m^3 of woody debris is estimated to still be resident within the catchment in locations vulnerable to remobilisation in a future storm event (Cave 2018a).

On 11th to 12th June 2018, a further 270 mm of rain fell in 48 hours north of Gisborne (Uawa and Mata catchments) causing additional land sliding, and reactivation and remobilization of landslides and landslide debris from the storm a week earlier. While peak rainfall intensities were lower than the first storm, the duration of intense rainfall was longer and the distribution more widespread (Cave 2018a).

A GeoNet landslide aerial reconnaissance was flown on 11th July 2018 by Brenda Rosser and Dougal Townsend of GNS, and Murry Cave of GDC. The results of this reconnaissance are included in this report. As part of the GeoNet landslide response, satellite imagery was obtained for some of the area affected by the storms.

Murry Cave of GDC requested a proposal from GNS Science to investigate the volume of sediment entering the Uawa River from landslides triggered by the rainstorms. This report covers both the GeoNet Landslide response and the GDC request.

1.1 Purpose of The Report

The objectives for the project as set out in the contract are to:

1. Determine the areas of erosion and deposition associated with the June 5th storm in the Uawa catchment, using differencing of satellite imagery;
2. Estimate the volume of sediment mobilised by landslides during the event, and
3. Calculate the sediment delivery ratio of landslides, and the volume of sediment that entered the Uawa River system.

GDC was also interested in whether differencing analysis pre- and post-event satellite imagery could provide a rapid and cost-effective tool for providing a credible quantification of the environmental impact of land sliding resulting from severe storms.

This report provides both the results of this study and the associated GIS data used and generated during the analysis. It has been prepared by GNS Science for Gisborne District Council with funding from Envirolink and GeoNet, in collaboration with Murry Cave, Principal Scientist, Gisborne District Council.

1.2 Data Sources

Gisborne District Council provided high-resolution aerial photographs taken in the summer of 2017/2018, prior to the rainstorm (0.3 m resolution GDC also provided data and analyses from their network of 59 rain gauges for the two rainfall events. Additional rainfall data from the MetService weather radar network was also accessed and used in the analysis. GDC also provided shapefiles of areas of recently logged exotic forest in the Uawa catchment.

GNS through the EQC-funded GeoNet Project funded acquisition of satellite imagery from Planet's Dove and SkySat satellite platforms for use in the analysis. The geology base layer used was from Mazengarb and Speden (2000) who mapped the geology of the Raukumara Peninsula at a scale of 1:250,000 for Qmap, the updated 1: 250,000 geological map of New Zealand.

Data on the erosion terrains was provided by Manaaki Whenua (Landcare Research). Land cover data (LCDBv4.1) was downloaded from Koordinates NZ (https://koordinates.com/).

2.0 JUNE 2018 STORM EVENTS

Gisborne District Council (GDC) has produced two reports describing the rainfall associated with the June 2018 storm events (Cave 2018a, Cave 2018b). The rainfall data for the East Coast - Tairawhiti Region was based on records from 59 rain gauges distributed across the area from Hicks Bay in the north to the top of the Wharerata Hills in the south, and rain radar data from MetService. Rainfall data from the storms are summarised below.

2.1 3rd to 4th June 2018

The first storm of 3rd and 4th June 2018 approached from the northwest and moved in a southeast direction across the East Coast - Tairawhiti region. The storm duration was approximately 12 hours, with most of the rain falling in a six to eight-hour period, ending about 8.30 am on the 4th June 2018. There was a narrow band of high intensity rainfall that hit the Uawa and Pakarae catchments at around 2.30 am on the 4th June 2018 (Figure 2.1 and Figure 2.2).

The storm was a moderate event with a narrow band of more intense rainfall affecting parts of the Uawa and Pakarae catchments. The highest intensity rainfall was recorded at the Panikau-Reed Road rain gauge located to the south in the adjacent Pakarae Catchment (Table 1; Figure 2.1), where 266 mm fell in 24 hours and a maximum intensity of 60.5 mm/hr was recorded. The highest rainfall in the Uawa catchment was recorded by the Mangaheia at Willowbank rain gauge, where 234 mm fell in 24 hours and a maximum intensity of 55.5 mm/hr was recorded Table 2.1; Figure 2.1). The annual return interval (ARI) for the 24-hour rainfall in the Uawa catchment at Willowbank was 12 years (Cave 2018a). The 1, 6 and 12-hour rainfall totals had higher ARI's of 50, 70 and 25 years respectively (from NIWA's High-intensity Rainfall Design System (HIRDS)). Other rain gauges in the Uawa Catchment recorded much lower rainfall with ARI's of around <2-5 years.

Table 2.1 Rainfall data for the June 2018 rainstorms in the Uawa and Pakarae catchments (Data from GDC).

Date	Rain gauge	Catchment	1 hr max	6 hr max	12 hr max	24 hr max	ARI 24hr
3rd – 4th June 2018 storm	Mangaheia at Willowbank	Uawa	55.5 mm	174.5 mm	202.5 mm	234.0 mm	12 years
	Panakau Rd – Reed Rd	Pakarae	60.5 mm	201.5mm	238.5 mm	252.5mm	32 years
11th – 12th June 2018 storm	Mangaheia at Willowbank	Uawa	9.5 mm		64.5 mm	89.5 mm	
	Panakau Rd – Reed Rd	Pakarae	15.0 mm		75.0 mm	108.0 mm	
	Tuahu	Uawa				173.5 mm	
	SH35 Bridge, Uawa River	Uawa				60.0 mm	

GDC provided contoured rain-gauge data for the 8-hour maximum rainfall (Figure 2.1). Gauge corrected rain radar from MetService (Figure 2.2) is consistent with the rain-gauge data and shows that the 12-hour maximum rainfall (i.e., encompassing the 6 to 8-hour rainfall event) is tightly confined to a narrow band starting at the southern boundary of the Pakarae catchment in the south and terminating at Mangaheia in the Uawa catchment (Cave 2018a).

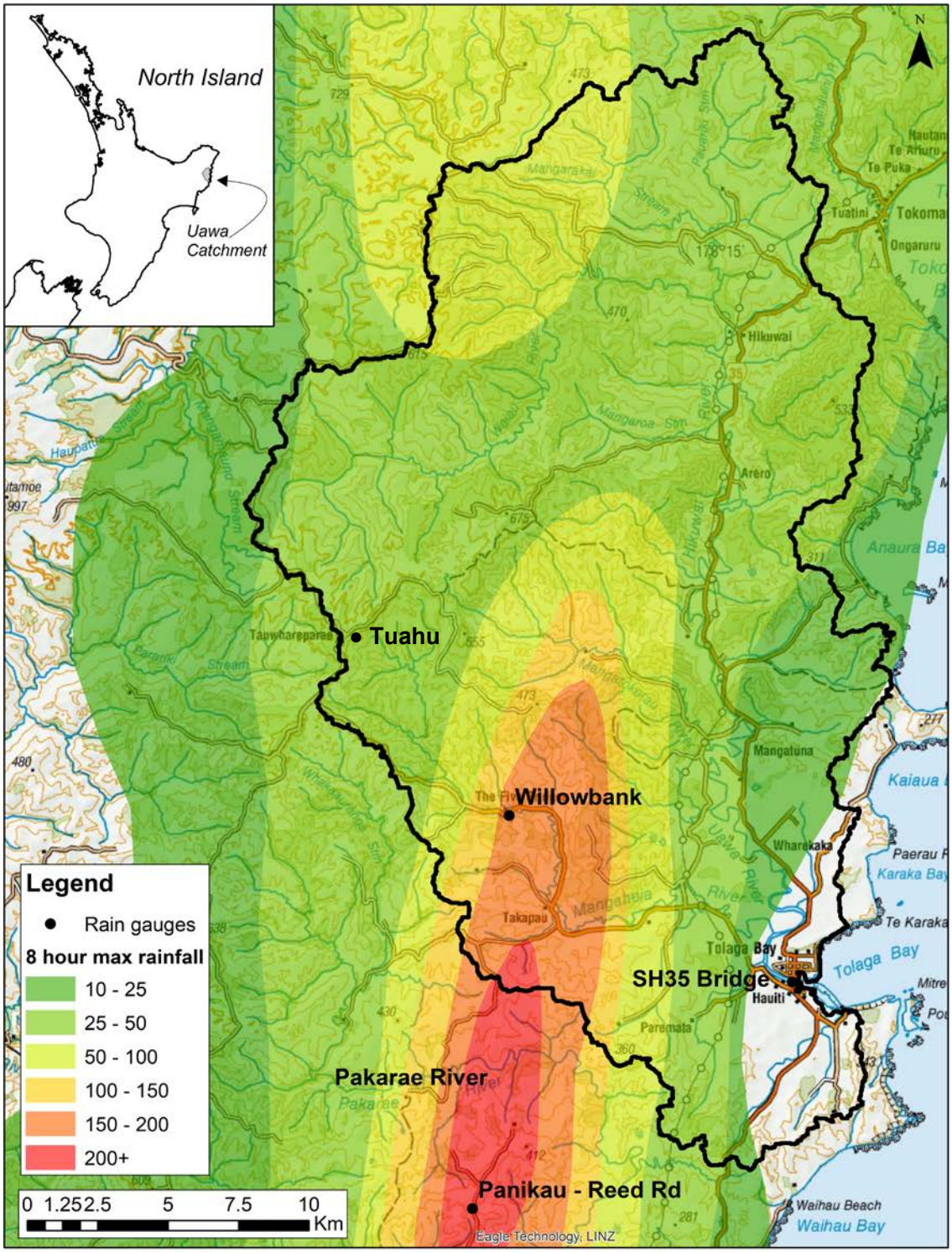

Figure 2.1 Contoured rain gauge data from GDC showing the 8-hour maximum rainfall, which encompasses the main storm event as recorded by rain-gauges at Panikau-Reed Road (in the Pakarae catchment) and Mangaehia at Willowbank (in the Uawa catchment). This contour plot is based on point rainfall data and interpolation between adjacent rain-gauges. The Uawa catchment is outlined in black.

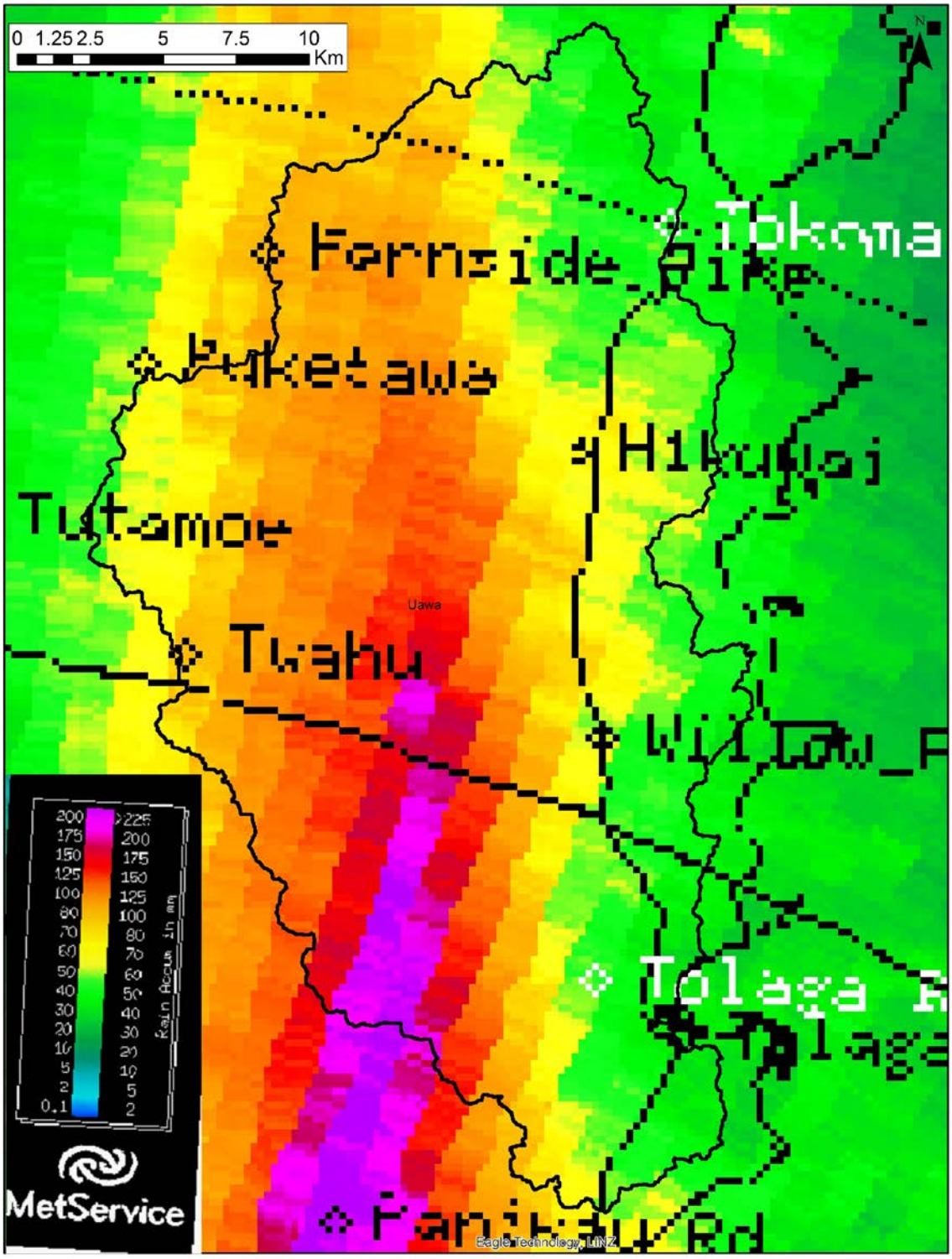

Figure 2.2 12-hour rain radar data from MetService.

2.2 11th to 12th June 2018

The June 11-12th storm was driven by a sub-tropical low centred over Bay of Plenty that moved south over the region. It brought heavy rain to the north of the Gisborne region, particularly in the northern Wharekahika and Waiapu Catchments. The storm had a duration of 24 hours, beginning around 1pm on the 11th June and ending by midday on the 12th June, and resulted in significant flooding events in the Waipaoa and Waiapu Rivers. Peak rainfall accumulations occurred at two rain gauge sites, the Raparapaririki in the Waiapu catchment (225.4 mm in 24 hrs), and at Waikura in the Hangaroa catchment (216 mm in 24 hrs), a tributary to the Wairoa River, to the south of the Waipaoa catchment. Rainfall was much lower in the Uawa catchment (Table 2.1). This storm caused some additional localised landslides in the Uawa catchment. Closed canopy (mature) forests were generally not affected. Some reworking and remobilisation of landslides triggered by the earlier, Queen's birthday storm was observed by GDC (Cave 2018b).

3.0 STUDY AREA

The Uawa Catchment covers 559 km^2 near Tolaga Bay, north of Gisborne (Figure 2.1). The catchment is underlain by poorly consolidated, Tertiary-age, sedimentary rocks that are susceptible to erosion. Erosion processes correlate with geology (Marden et al 1991), and rainfall-induced soil slides, debris slides and debris avalanches dominate steep slopes in the catchment. Deep seated rotational slumps, earthflow and gullies are present, but are less prevalent than the shallow soil slides, flows and avalanches (Marden et al 1991). Valleys are deeply dissected, with steep, north-facing scarp slopes and less steep south-facing dip slopes. Soils were originally developed in late-Quaternary volcanic ash (Marden et al 1991). Soils are thin (0.1 to 0.5 m) on scarp slopes where tephras have often been removed by erosion, and thicker on dip slopes where tephras have been preserved.

Mean annual rainfall in the catchment varies from 700 mm/year at the coast to 2500 mmm/year in the headwaters. Droughts are common during January to April and the area has a history of severe storms, many of which begin as Tropical Cyclones (Marden et al 1991). The highest recorded rainfall in the Uawa catchment was during Cyclone Bola in 1988, when more than 900 mm was recorded over five days (Marden et al 1991). Two recent ex-tropical cyclones, Ex-Tropical Cyclone Cook and Ex-Tropical Cyclone Debbie, both occurring in April 2017, caused landslide damage in the Uawa catchment, and mobilised woody debris (Cave et al. 2017).

3.1 Geology and Geomorphology

Hillslopes in the Uawa catchment are underlain by two geological units (Figure 3.1):

1. Tolaga Group: Miocene-age mudstone and sandstone
2. Mangaheia Goup: Late Miocene – Pliocene-age mudstone and sandstone

Statistics on the coverage of the two units in the Uawa catchment from the Mazengarb and Speden (2000), 1:250 000 geological map are given in Table 3.1. Other geological units in the catchment include Late Pleistocene and Holocene sediments of the floodplains, alluvial terraces and fans and small isolated areas of East Coast Allocthon and Late Cretaceous - Early Miocene melange.

Table 3.1 Statistical data for geological units in the Uawa catchment based on the mapping of Mazengarb and Speden (2000).

Geological Unit	Area (km^2)	% of catchment
Tolaga Group	364.7	65.2
Mangaheia Group	120.2	21.5
Holocene sediments	70.6	12.6
East Coast Allochthon	2.8	0.5
Late Pleistocene sediments	0.5	0.1
Late Cretaceous - Early Miocene melange	0.5	0.1
Total	**559.2**	**100.0**

Landforms within the Uawa catchment are based on Land Use Capability (LUC) units from the New Zealand Land Resource Inventory (NZLRI) (Lynn et al 2009), grouped according to slope (Figure 3.2). Most of the catchment is steep hill country and hilly steep lands (LUC units 5, 6 and 7) underlain by weak to very weak Tertiary sedimentary rocks where mass movement

processes are common (Figure 3.2). For the purpose of this report, all rapid mass movement processes including soil slides, debris slides, debris flows, and debris avalanches are analysed together under the term landslides.

3.2 Erosion Terrains

New Zealand erosion terrains were defined by researchers at Landcare Research in the 1990's. They are based on rock type groupings of Land Use Capability units in the New Zealand Land Resource Inventory (NZLRI) (Page et al 1999). The erosion terrains define land in New Zealand by the erosion processes operating on different rock types, using landform, slope angle and rainfall as distinguishing characteristics (Dymond et al, 2010). A three-level hierarchical classification was developed. At the top level, terrains were differentiated based on landform and slope. At the second level, groups were defined on rock type. And at the third level, groups were differentiated by erosion processes and further differentiation of rock type (Dymond et al 2010).

The erosion terrains are used here because previous work in the adjacent Waipaoa catchment (Page et al 1999, Reid and Page 2002) provided data on landslide dimensions (area, depths, volume) and sediment delivery (Reid and Page, 2002) that can be applied to landslides on similar erosion terrains in the Uawa catchment. Page et al (1999) provided detailed descriptions of the erosion terrains in the Waipaoa catchment including their susceptibility to erosion, and the types of erosion that occur. In the Waipaoa catchment local names were assigned to erosion units for a typical area where the units were located (Page et al 1999). Subsequently a numbering system has been developed and applied nationwide (Dymond et al 2010).

We correlated the erosion terrains defined by Page et al (1999) for the Waipaoa catchment with rock types in the Uawa catchment (Table 3.2). The location of the erosion terrains in the Uawa catchment are shown in Figure 3.3. Descriptions of the erosion terrains present in the Uawa catchment are listed in Table 3.3.

3.3 Land Cover

The vegetation classes in the Uawa Catchment were mapped during the summer 2012/13 for the Landcover Database version 4.1 (LCDB v4.1) and are shown in Figure 3.4. The areas occupied by each class are listed in Table 3.4. The planting of exotic forests accelerated in the area from 1980, in response to widespread erosion in catchments (Marden et al 1991). Planting of exotic forest was funded under various Government schemes that provided incentives for afforestation of highly erodible land and targeted Land-Use Classes (LUC) 6 to 8 (Marden et al 1991).

GDC provided shapefiles of areas of harvested commercial forest since LCDB v4.1 was published. These areas were subtracted from areas of 'Forestry' identified in the LCDB v4.1 data. Areas of plantation forestry harvested have been divided into two groups; areas harvested at the time of LCDBv4.1 mapping, and areas harvested from 2013 to 2018. These areas are considered vulnerable to erosion during high intensity or prolonged rainfall (Marden et al 1991). Most areas of commercial forestry are probably in their second logging cycle (Murry Cave pers. comm.).

Table 3.2 Relationship between Waipaoa erosion terrains (Page et al, 1999) to the Uawa catchment geology (Mazengarb and Speden, 2000) where applicable. The total percentages do not add to 100 nor do they match the geology percentages given in Table 3.1 because the erosion terrains are based on the mapping units and rock type classification of the NZLRI (Lynn and Crippen 1991).

Waipaoa catchment erosion terrains	Uawa catchment geology	Erosion terrain codes	% catchment
Te Arai (+ Waingaromia)	Tolaga Group (+ Crushed and sheared Tolaga Group) Earthflow and gully dominated Small areas of East Coast Allocthon and Melange	6.4.1, 7.3.1, 6.4.2, 6.4.3, 6.4.4, 7.3.2	59.6
Wharerata	Mangaheia Group	6.4.5 and 7.4.1	20.7
Wharekopae	Mangaheia Group (tephra mantled)	5.2.3 and 6.2.4	6.7
Waipaoa	Holocene alluvial deposits and Late Pleistocene river and terrace deposits	1.1.1, 2.1.2, 3.1.1, 4.1.1, 4.2.4	12.7

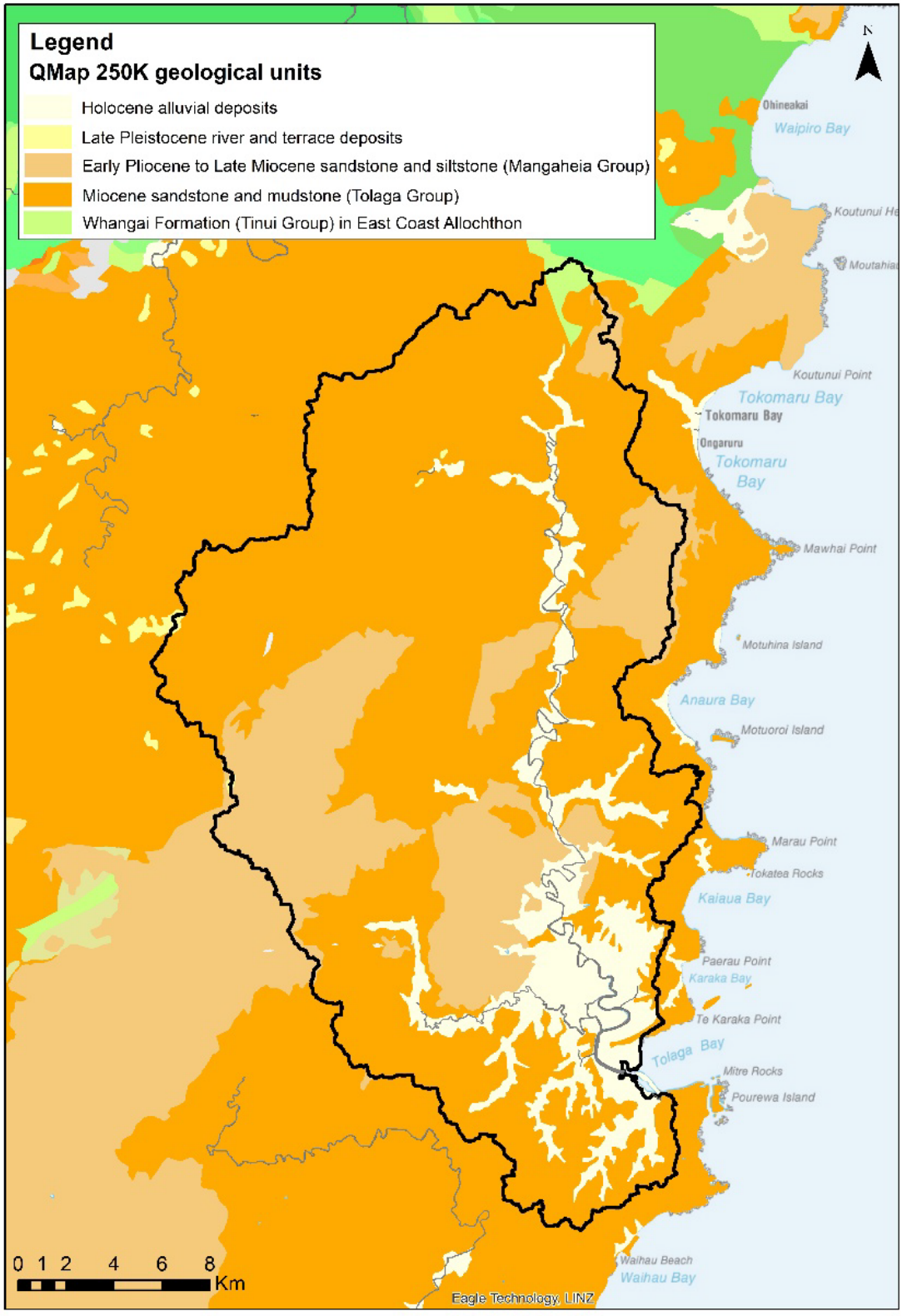

Figure 3.1 Simplified geology of the Uawa catchment (from Mazengarb and Speden, 2000).

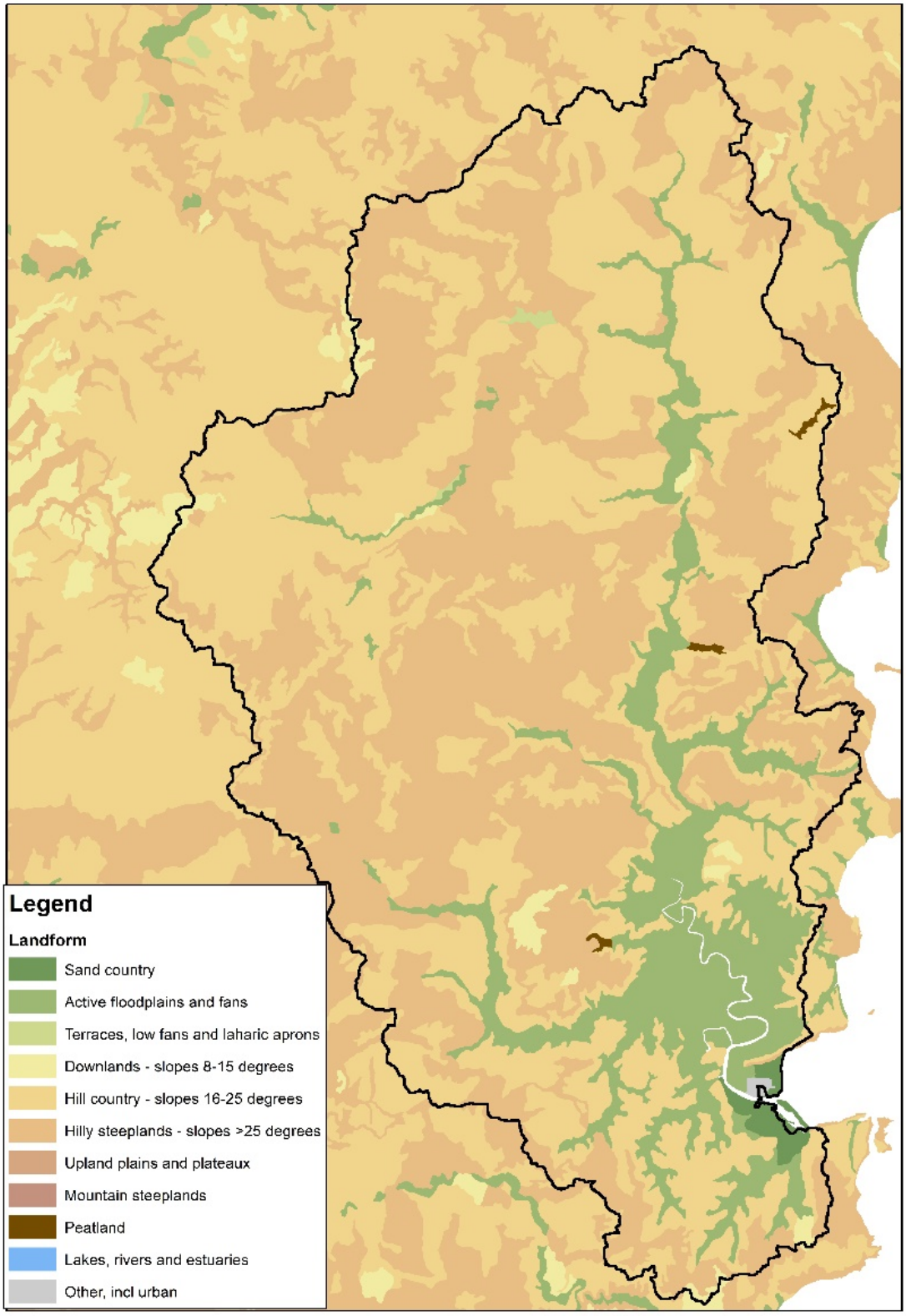

Figure 3.2 Landforms in the Uawa catchment. The landforms were taken from the Land Use Capability units in the NZLRI (Lynn et al 2009) and differentiated by slope (Dymond et al 2010).

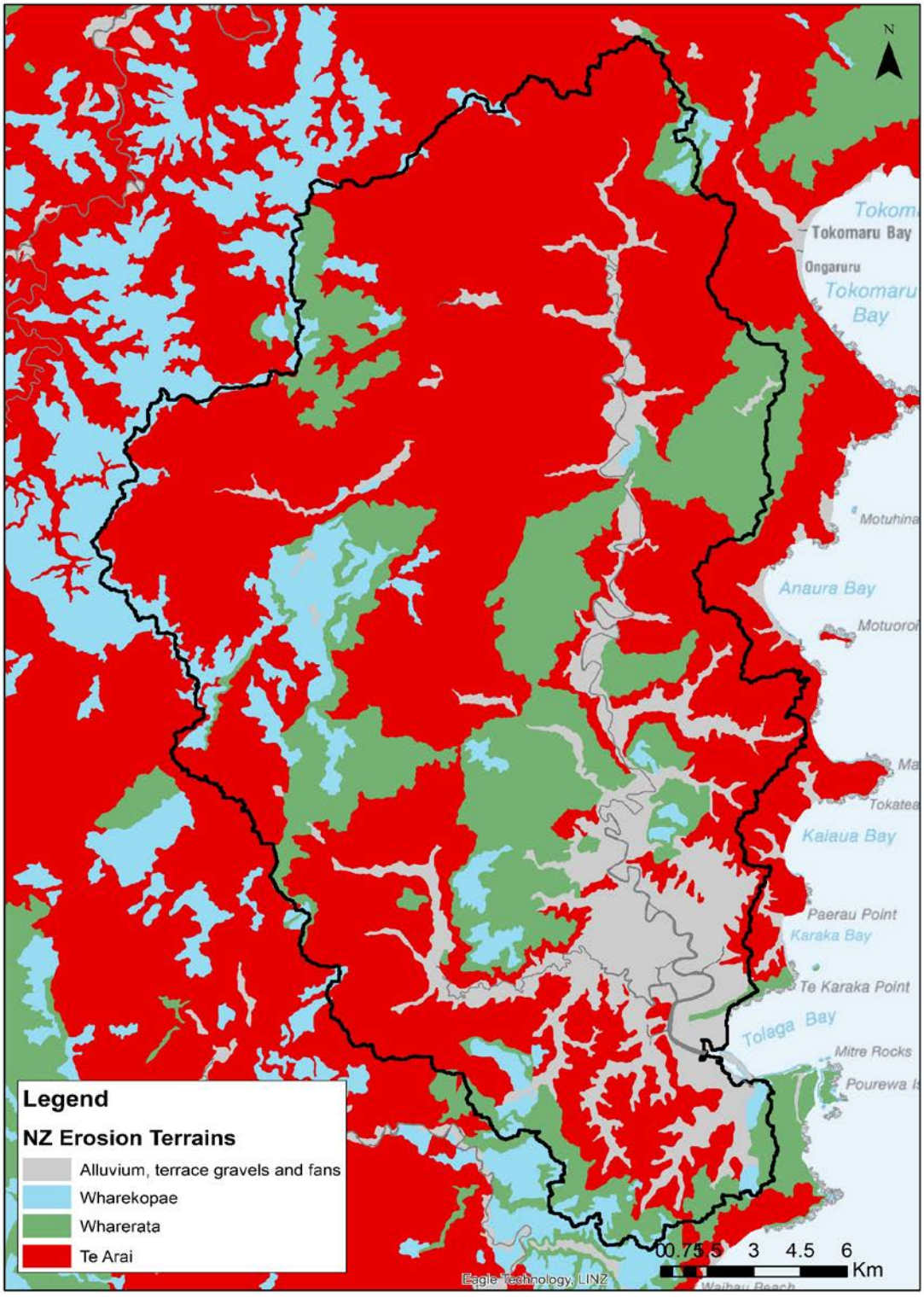

Figure 3.3 Distribution of erosion terrains in the Uawa catchment. For simplicity, the original names from the Waipaoa catchment have been used. The corresponding Erosion terrain codes are listed in Table 3.3.

Table 3.3 Erosion terrain descriptions for the Uawa catchment.

Name	Erosion terrain code	Area (km^2)	% area	Description
Alluvium	1.1.1	71.4	12.8	Undifferentiated alluvium from modern overbank depositional events. Parts may be peaty. Includes non-peaty wetlands
Sand	2.1.2	3.0	0.5	Recent fresh dune sand
Peat	3.1.1	0.8	0.1	Organic soils on deep peat
Terraces	4.1.1	0.6	0.1	Gravelly soils on alluvial terrace gravels above the level of modern flood plain
Terraces and fans	4.2.4	0.2	0.0	Terraces and fans of mid-aged (late Pleistocene/early Holocene) tephra, older tephra, or tephric loess
Wharekopae	5.2.3	5.7	1.0	Downlands developed on Mid-aged (late Pleistocene/early Holocene) tephra, older tephra, or tephric loess
Wharekopae	6.2.4	31.6	5.7	Hill country developed on Mid-aged (late Pleistocene/early Holocene) tephra, or tephric loess, covers
Wharerata	6.4.5	22.4	4.0	Hill country developed on weak to moderately strong Tertiary-aged sandstone
Wharerata	7.4.1	93.2	16.7	Hilly steeplands developed on cohesive, generally weak to moderately strong Tertiary-aged sandstone
Te Arai	6.4.1	85.8	15.3	Hill country developed on weak to very weak Tertiary-aged mudstone
Te Arai (Waingaromia)	6.4.2	0.3	0.1	Hill country developed on crushed Tertiary-aged mudstone, sandstone; argillite, or ancient volcanic rock (frequently, with tephra covers in the Northern Hawke's Bay–East Coast area) with moderate earthflow-dominated erosion
Te Arai (Waingaromia)	6.4.3	37.4	6.7	Hill country developed on crushed mudstone or argillite with severe earthflow-dominated erosion. Includes small areas of Late Cretaceous to Early Miocene melange
Te Arai (Waingaromia)	6.4.4	68.5	12.3	Hill country developed on crushed argillite, sandstone, or greywacke, with severe gully-dominated erosion
Te Arai	7.3.1	134.9	24.1	Hilly steeplands developed on weak to very weak Tertiary-aged mudstone
Te Arai (Waingaromia)	7.3.2	2.7	0.5	Hilly steeplands developed on crushed argillite with gully-dominated erosion. Includes small areas of East Coast Allocthon
Total		**559.0**	**100**	

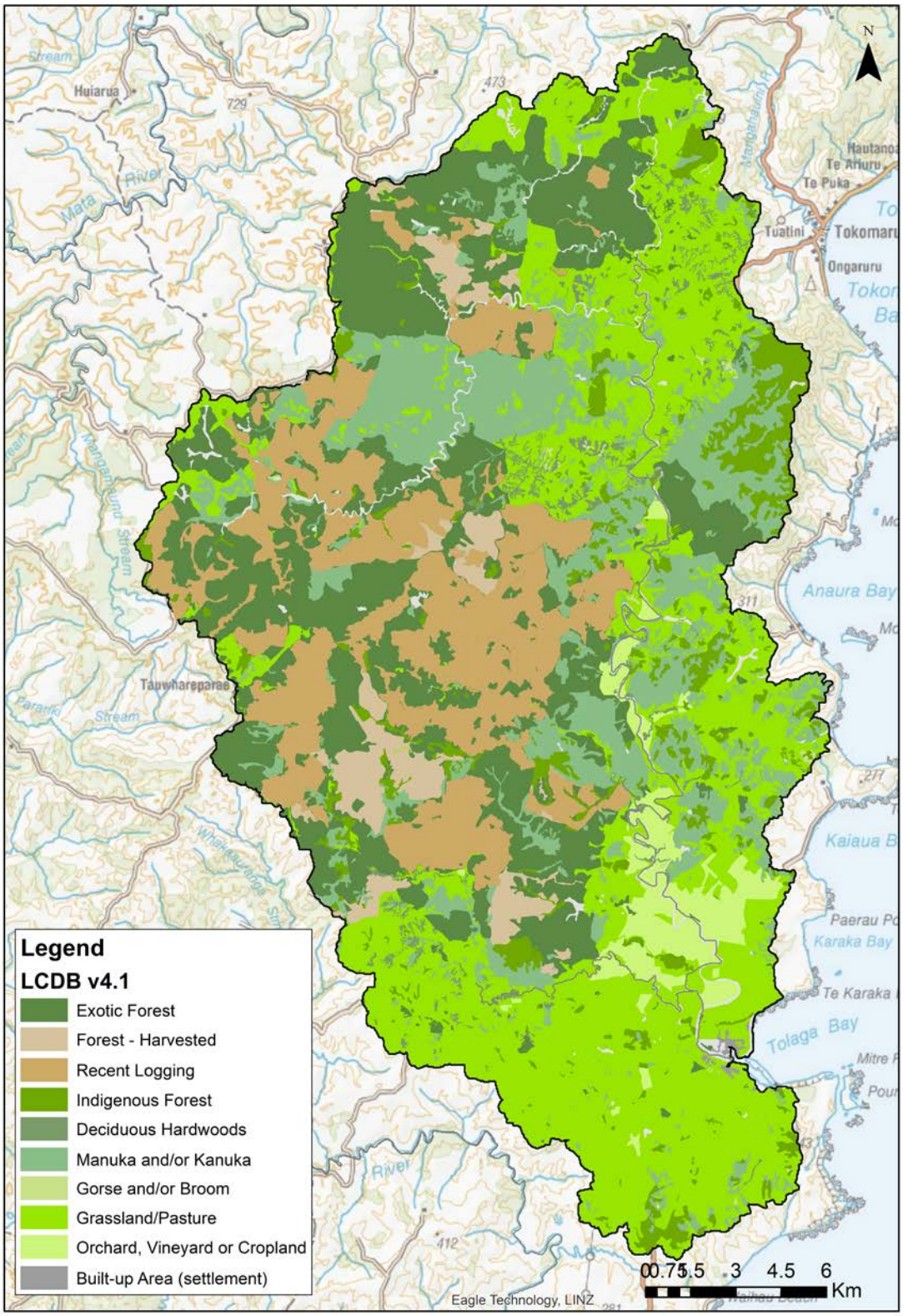

Figure 3.4 Distribution of land cover classes in the Uawa catchment from the LCDBv4.1, as mapped in 2012/13. Areas of harvested forest have been divided into two groups, areas harvested before 2013 and areas harvested between 2013 and 2018 (recent). Recent forestry harvest areas were provided by GDC.

Table 3.4 Land cover vegetation classes in the Uawa catchment (from LCDB 4.1, mapped in 2012/13). Areas of recently harvested forest (2013--2018) were provided by GDC.

Vegetation Class	Area (km^2)	%
Exotic Forest	111.9	20.0
Forest – harvested before 2013	25.0	4.5
Forest – harvested 2013-2018	90.6	16.2
Grassland/Pasture	174.9	31.2
Manuka and/or Kanuka	88.6	15.8
Indigenous forest	32.7	5.8
Cropland	18.8	3.4
Deciduous Hardwoods	7.9	1.4
Gorse/Broom	0.7	0.1
Other	0.7	1.6
Total	**560.1**	**100.0**

4.0 LANDSLIDE RECONNAISSANCE

4.1 Landslide Types and Examples

A GeoNet landslide response was undertaken by Brenda Rosser and Dougal Townsend of GNS Science, and Murry Cave of GDC on 11th July 2018. The following photos taken during the reconnaissance flight document the landslides caused by both events. The predominant landslide types triggered were shallow (~1m depth) translational soil slides, debris slides and debris flows, in areas recently harvested (Figure 3.4). The landsides mostly initiated in gully heads or along ridge crests (Figure 4.1 and Figure 4.2). The highest number of landslides were observed in recently harvested or re-planted areas (Figure 4.1 to Figure 4.3), but landslides also occurred in established pine plantations (Figure 4.4). Landslide terminology used here is as described by Hungr et al (2014).

Some of the larger soil slides and debris flows were associated with roads, landings and skid platforms constructed to enable forest harvest activities. Several occurred in areas of closed canopy forest (mature forest) probably on their second crop rotation (Murry Cave pers. comm.) (Figure 4.4 and Figure 4.5). In recently harvested areas many of the landslide source areas, originated from disturbed ground (mostly fills) associated with the roads, landings and skid platforms (Figure 4.6 to Figure 4.10). If the landings and roads are constructed with poor practices (side-cast or end-tipped fill construction techniques) they can be more vulnerable to slope failure during high-intensity rainfall and because woody material from logging operations is often left on these fill slopes this can then be entrained and mobilised in landslides, debris slides and debris flows (Bloomberg et al 2011). Many landslides occurred along forestry roads in the cut slope above the road, or in the fill slope below (Figure 4.11 and Figure 4.12).

There were some shallow soil slides on pasture but areas in pasture were visibly less affected than areas of recently harvested forest (Figure 4.11). There were a few larger rotational slumps observed (Figure 4.14), however, this failure mechanism was not identified regularly across the study area. In some cases, sediment and woody debris generated by landslides was delivered directly to stream channels (Figure 4.15). In other locations, some landslide material remained stored on the slopes. Lots of woody debris was observed stored in first order stream channels (Figure 4.16). There was some bank erosion observed in the downstream reaches of the Mangaheia and Uawa Rivers (Figure 4.17). No survey of the river and stream channel erosion was undertaken so no estimate can be made of the amount of sediment generated by bank erosion.

4.2 Downstream Deposition and Impacts

A notable impact of the Queen's Birthday storm event was woody debris and sediment deposition on floodplains in the lower reaches of the major rivers (Hikuwai, Uawa, Mangatokerau, Mangaheia) (Figure 4.16 to Figure 4.20) and on the beach at Tolaga Bay (Cave 2018a). GDC calculated that 47,000 m^3 of logs were deposited on Tolaga Bay beach following the storm (Cave 2018a). This does not include the thousands of cubic meters of woody debris remaining on the slopes, in first-order streams (Figure 5.2) or stored on the floodplains of the main rivers (Figure 4.16 to Figure 4.19). Debris floods and flows occurred in many of the river and stream channels downstream of the landslides and were likely the mechanism that transported the woody debris from the headwater catchments downstream to the floodplain and coast at Tolaga Bay.

Figure 4.1 Extensive shallow soil slides, debris slides and debris flows, on newly harvested areas in the headwaters of the Mangatoitoi (Uawa Forest) (D. Townsend, GNS Science; 11 July 2018; D85_7882).

Figure 4.2 Extensive shallow soil slides, debris slides and debris flows in a newly forested area in the Mangatoitoi stream tributary of the Mangaheia River (Uawa Forest) (D. Townsend, GNS Science; 11 July 2018; D85_8017).

Figure 4.3 Extensive shallow soil slides, debris slides and debris flows in a newly forested area in the upper Takamapohia Stream, Te Mauranga Forest, Mangatokerau catchment (D. Townsend, GNS Science; 11 July 2018; D85_7844).

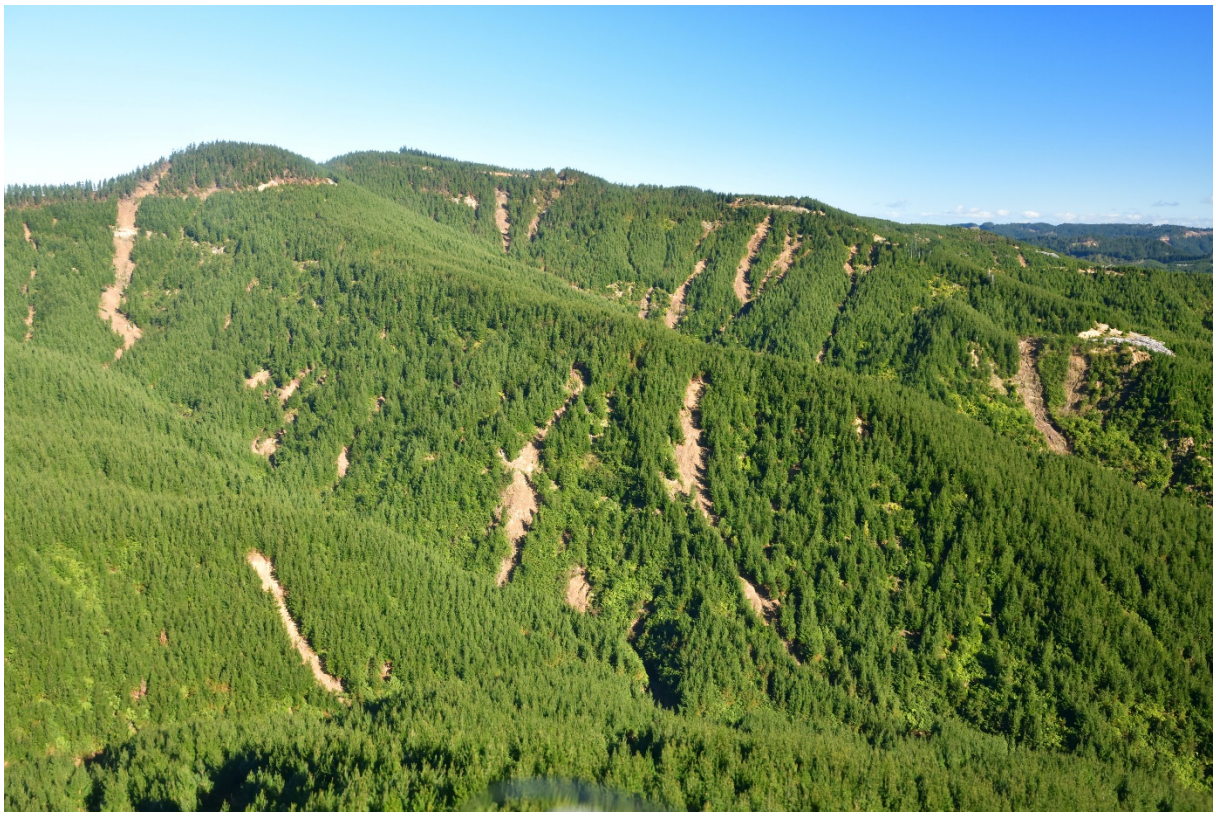

Figure 4.4 Debris slides and debris flows in established maturing forests in the headwaters of the Waiau River (tributary of the Hikuwai River). Some of these may have their source areas associated with forest harvest infrastructure such as roads and landings (D. Townsend, GNS Science; 11 July 2018; D85_7830).

Figure 4.5 Debris flows initiated in established pine plantations in the headwaters of the Mangatokerau River (Te Mauranga Forest). The right-hand debris flow may have initiated in fill associated with the water reservoir visible on the ridge crest (D. Townsend, GNS Science; 11 July 2018; D85_7879).

Figure 4.6 Skid haul operation in a newly harvested area in the head of Tapaue Stream, Paroa Forest, Uawa catchment. Shallow soil slides have initiated in the fill slopes constructed for landings and roads built to facilitate harvesting operations (D. Townsend, GNS Science; 11 July 2018; D85_7887).

Figure 4.7 Shallow soil slides and debris flows with source areas in fill slopes below a landing on recently logged slopes in the headwaters of Takamapohia Stream, tributary of the Mangatokerau River (Te Mauranga Forest) (D. Townsend, GNS Science; 11 July 2018; D85_7836).

Figure 4.8 Soil slides and debris flows with source areas in fill used to construct a landing in the Mangatoitoi Stream, Mangaheia catchment near Five Bridges (Uawa Forest) (D. Townsend, GNS Science; 11 July 2018; D85_8035).

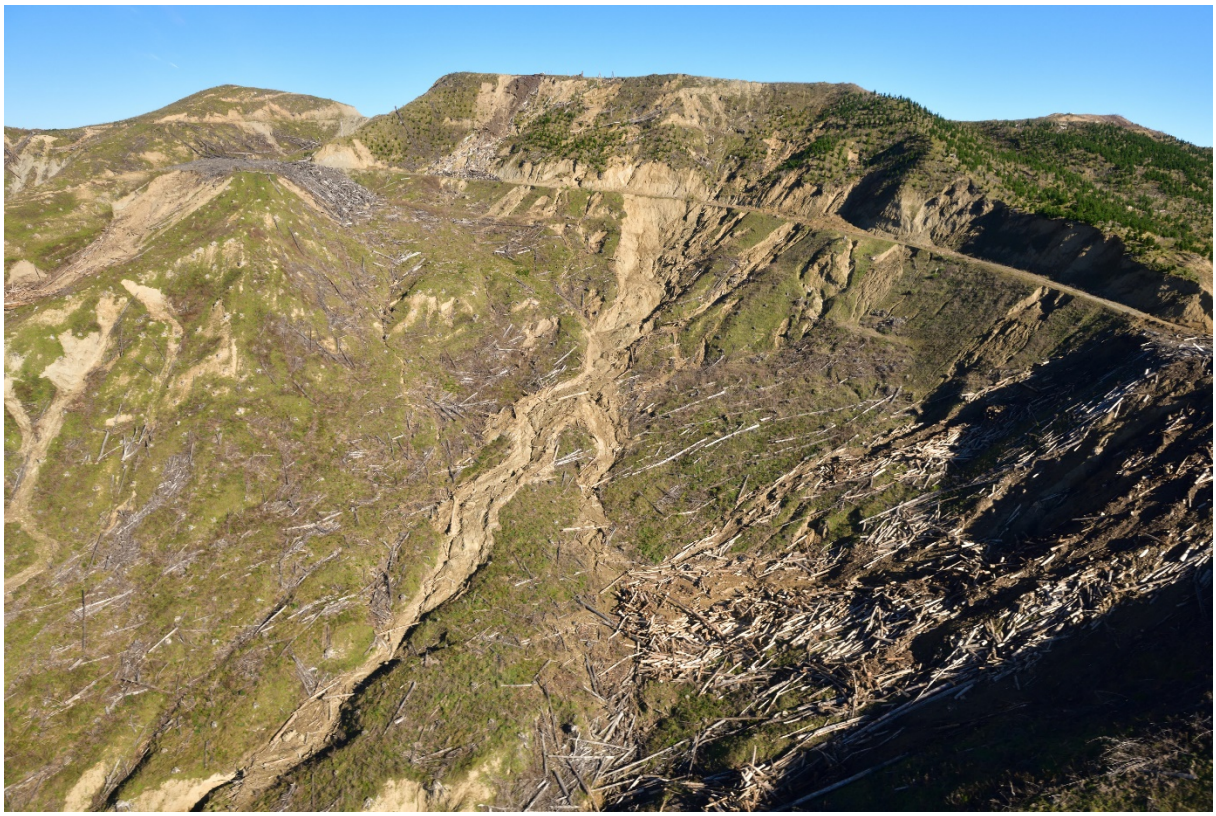

Figure 4.9 Debris flow initiated in the fill slope of a forestry road in the head of Mangatoitoi Stream, Mangaheia catchment near Five Bridges (Uawa Forest). Also obvious are many smaller rock-falls, soil-falls, rock slides and soil slides that initiated on or above the cut slope associated with the road (D. Townsend, GNS Science; 11 July 2018; D85_8026).

Figure 4.10 Soil and rock falls, soil and rock slides, and soil flows originating on or above cut slopes above Tirohanga forestry road between Kaimonona and Te Kokokakahi Streams in the headwaters of Mangatokerau River (D. Townsend, GNS Science; 11 July 2018; D85_7872).

Figure 4.11 Largely unaffected pasture on hilly steep lands developed on cohesive, generally weak to moderately strong Tertiary-aged rocks in the headwaters of the Waiau River west of Fernside Road (D. Townsend, GNS Science; 11 July 2018; D85_7816).

Figure 4.12 Large rotational slump in the headwaters of Waiau River east of Fernside Road (tributary of Hikuwai River) (D. Townsend, GNS Science; 11 July 2018; D85_7817).

Figure 4.13 Debris slide directly coupled to the channel of the Mangaheia River, on Drysdale forestry road above Five Bridges. Sediment and woody debris have been delivered directly to the channel (D. Townsend, GNS Science; 11 July 2018; D85_8043).

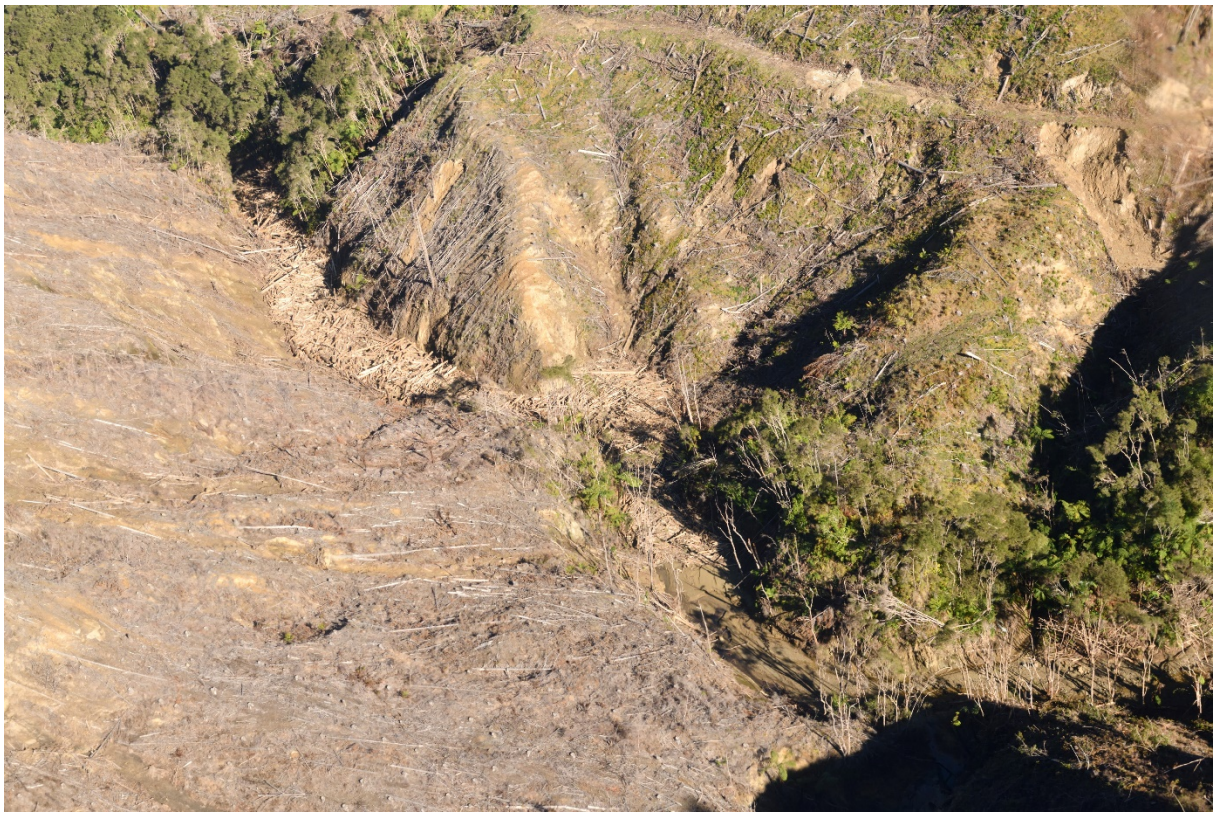

Figure 4.14 Woody debris generated from logging activities and transported by shallow soil slides, debris slides and debris flows stored in first order stream channels in the headwaters of Tapaue Stream, Paroa Forest, Uawa Catchment. (D. Townsend, GNS Science; 11 July 2018; D85_7894).

Figure 4.15 Bank erosion in the middle reaches of the Mangaheia River, downstream of Takapau Road/Wigan Bridge (D. Townsend, GNS Science; 11 July 2018; D85_7970).

Figure 4.16 Woody debris deposited on the floodplain of the Mangatokerau River upstream of the Paroa Road Bridge showing Mangatokerau Road where 3 people were rescued during the Queen's Birthday Storm (D. Townsend, GNS Science; 11 July 2018; D85_7913).

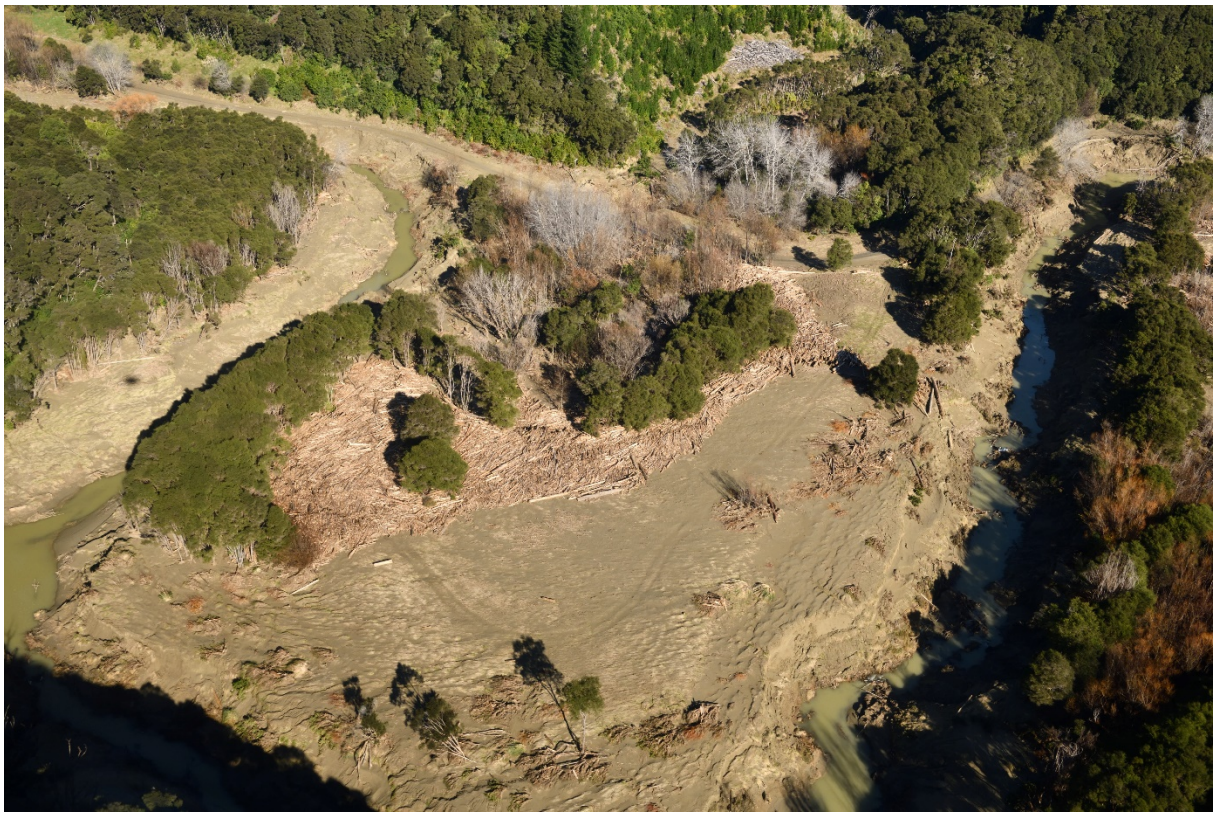

Figure 4.17 Woody debris deposited on the floodplain of the Mangatokerau River downstream from Mangatokerau Road (D. Townsend, GNS Science; 11 July 2018; D85_7932).

Figure 4.18 Sediment and woody debris deposited on the Tapaue Stream floodplain on Paroa Station (D. Townsend, GNS Science; 11 July 2018; D85_7946).

Figure 4.19 Sediment and woody debris deposited on the Tapaue Stream floodplain, Paroa Road (D. Townsend, GNS Science; 11 July 2018; D85_7960).

Figure 4.20 Sediment deposition on the floodplain of the Mangaheia River at Wigan Bridge (D. Townsend, GNS Science; 11 July 2018; D85_7978).

5.0 ASSESSMENT OF SATELLITE IMAGERY FOR LANDSLIDE MAPPING

5.1 Data Sources

A rapid regional-scale assessment of landslide severity was undertaken by comparing satellite imagery taken before and after the storms to identify and map new landslides. For this study, the pre- and post-storm images from the European Space Agency's Sentinel satellites and Planet's Dove and SkySat satellite constellations were used. Sentinel-2 Level-1C data the ESA Sentinel data hub (https://scihub.copernicus.eu), and Planet Level-3B Analytic MS data (Dove satellite data) was downloaded from https://www.planet.com/explorer/. Images were selected with minimal cloud cover but encapsulating immediate post-event damage. These images were already converted to display surface reflectance. Post-event imagery was also acquired from the Planet SkySat constellation and was used as a check on the automatic classification of landslides from differencing of Sentinel and Dove pre- and post-event satellite images. The extents of the various post-event satellite imagery available for the Uawa catchment are shown in Figure 5.1 and described in Table 5.1.

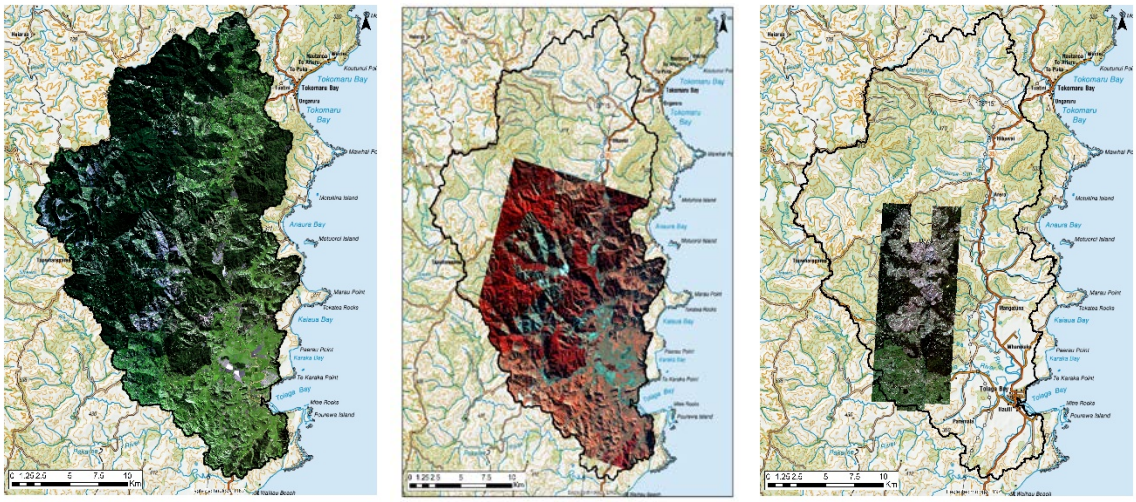

Figure 5.1 Extents of available post-storm satellite imagery: a) Sentinel, b) Planet Dove and c) Planet SkySat.

Table 5.1 Comparison of areas, resolution and mapping methods used for each type of Satellite imagery.

	Satellite		
	Sentinel	**Planet Dove**	**Planet SkySat**
Resolution	10 m	3 m	0.8 m
Area covered	560 km^2	452 km^2	111.5 km^2
Mapping method	Automated	Automated	Manual

5.1.1 Sentinel imagery

Sentinel-2 is the European Union operated earth observation mission and consists of a constellation with two identical satellites, Sentinel-2A and Sentinel-2B. Four bands in the visible/near infrared (VNIR) range are captured at 10m spatial resolution and were used here for landslide analysis (Table 5.2).

Table 5.2 Sentinel datasets used to for differencing.

Sr. #	Satellite	Image Date	Time (in UTC)	Remarks
1	Sentinel-2A	23 May 2018	22:06	Complete coverage of Uawa Catchment
2	Sentinel-2A	5 June 2018	22:06	Presence of cloud in the northern part of the catchment and no coverage of Tolaga Bay
3	Sentinel-2B	27 June 2018	22:16	Complete coverage of Uawa catchment

5.1.2 Planet Dove imagery

Planet is currently operating the largest constellation of miniature-sized (10cm x 10cm x 30cm) 'Dove' satellites for Earth observation at 3m spatial resolution. The Planet Dove images acquired from Planet for landslide detection are listed in Table 5.3.

Table 5.3 Images acquired from Planet's Dove satellite constellation for this analysis.

Sr. #	Satellite	Image Date	Time (in UTC)	Remarks
1	0f4b	19 May 2018	22:11	Partial coverage of Uawa Catchment
2	0f2d	13 June 2018	23:08	Limited coverage of the catchment. Late morning image capture time shows less topographic shadow which helps in better visual identification of landslides on south-facing slopes.
3	0f52	16 June 2018	21:35	No coverage in the northern and western areas of Uawa catchment. Early morning satellite pass causes poor visibility on south-facing slopes.

5.1.3 Planet SkySat imagery

SkySat is a constellation of sub-meter resolution Earth observation satellites also operated by Planet. Each SkySat satellite captures data in one panchromatic band (~80cm) and four multispectral bands (at 2m resolution) in the very near infra-red (VNIR) range. Post-event pan-sharpened images were available at sub-meter resolution (0.8 m) (Table 5.4). Post-event SkySat imagery was used for manual landslide mapping as a check on the accuracy of satellite differencing to identity new landslides (Section 5.2.3).

Table 5.4 Images acquired from Planet SkySat satellites.

Sr. #	Satellite	Image Date	Time (in UTC)	Remarks
1	SS-3	13 Sep 2018	21:57	Partial coverage of Uawa Catchment
2	SS-7	14 Sep 2018	00:48	Partial coverage, mid-day revisit (at maximum sun-elevation) resulting in minimum ridge shadowing effect in the image which is good for visual analysis

5.2 Mapping Methodology

5.2.1 Landslides

Landslide polygons were extracted using a semi-automated approach by comparing pre- and post-event images to identify pixels with visual changes. An automated extraction of potential landslide scars as polygon features using GIS was then undertaken to rapidly determine potential landslides. Given that fresh landslide scars, debris tails, and the presence of fine sediment on the floodplain appears bright and highly reflective when viewing the true-colour image, we used strong spectral differences between the pre- and post-event imagery to indicate recent landslide scars and overbank sediment deposition. By calculating the change in the pixel value across a single band (B04 Red), and extracting the pixels with highest variance, two polygon sets representing the landslide (scar plus debris tail) and downstream overbank deposition were generated. Due to the scale of the satellite imagery, it was not possible to differentiate between landslide source areas (scars) and deposits (debris tails).

The difference image (I_d) represents the pixel value difference in the form of simple digital number, the radiance or the reflectance value. The change in the difference image can be extracted by a simple thresholding. There are numerous ways to determine the threshold value either empirically or statistically, often empirical methods (such as linear or percentile based threshold values) generate better results (Singh, 1989). For both Sentinel and Planet datasets, a difference image was computed using only the red band because it is less sensitive to changes in vegetation. Three different threshold-based change images were generated which showed both negative and positive change. For Sentinel images, we used linear change thresholds of 5, 7.5, and 10 percent reflectance for differences between the pre- and post-event images. For Planet images, percentile change thresholds of 5, 10, and 15 percent reflectance were used. These thresholds were empirically derived after visual interpretation of landslides that occurred on forested, logged and pasture hillslopes.

It is important to note that there are other factors which can also influence the image difference (I_d) values such as differences in atmospheric conditions, sun angle and soil moisture (Jenson, 1983). Differences may also be introduced due to incorrect image registration resulting in a shift in the location of features in pre- and post-event imagery.

This dataset was manually checked and to remove potential errors (e.g. cloud cover), and each polygon was attributed as either landslide or deposition. The result was two sets of fresh bare ground polygons, representing the change between 23rd May 2018 and 27th June 2018 for Sentinel imagery, and 19th May 2018 and 13th June 2018 for Planet Dove imagery (Figure 5.2). Post-event imagery for all satellites were from after the 2nd storm. The assumption was made that landslides mapped here were triggered by the storm with the greatest rainfall (ie. the 3rd-4th June Queen's Birthday storm). GDC confirmed that there was some reactivation of landslides and reworking of landslide deposits during the June 11-12th storm, but this was minimal, and the majority of new landslides were triggered by the June 3rd-4th storm. River flow in the Uawa River and its tributaries was also confined to the channel in the June 11-12th storm (Murry Cave pers. comm).

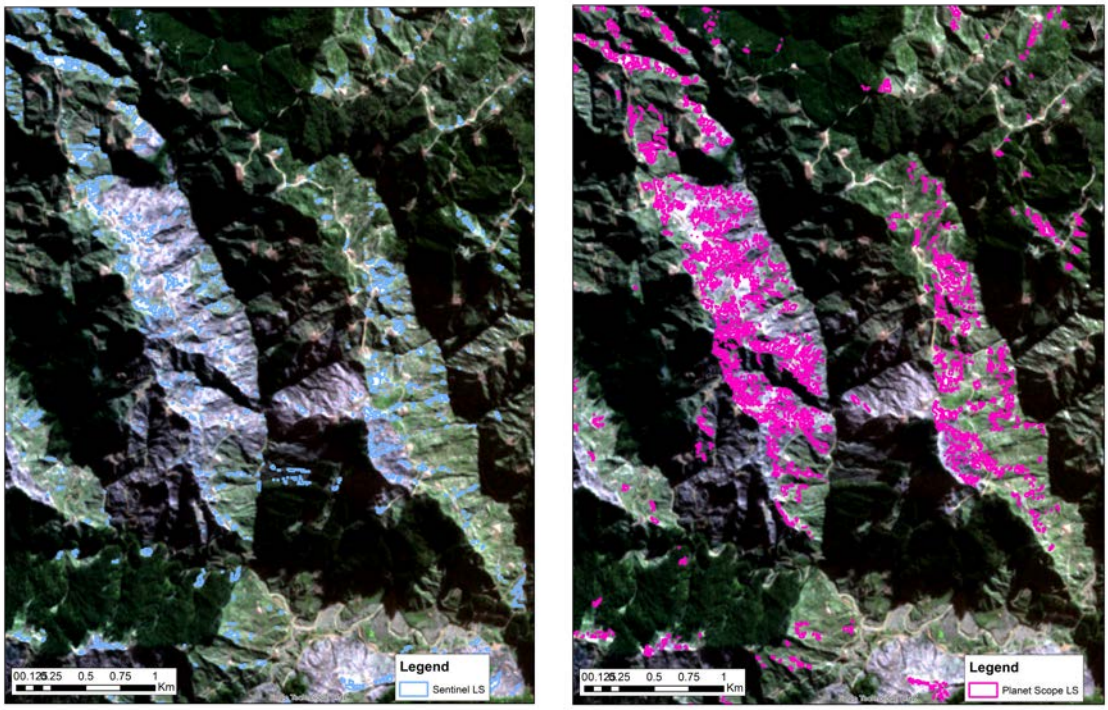

Figure 5.2 Mapped landslides from the Queen's Birthday storm in the Uawa catchment using automatic extraction of landslides from a) Sentinel and b) Planet Dove imagery differencing.

5.2.2 Overbank deposition

To detect the extent of overbank deposition associated with flooding and debris flows, we derived the Normalised Difference Water Index (NDWI) from pre- and post-event images. We used the following equation to determine NDWI from 10m resolution Sentinel and 3m resolution Planet images:

$$NDWI = \frac{\rho_{blue} - \rho_{nir}}{\rho_{blue} + \rho_{nir}}$$

where ρ is the reflectance of corresponding spectral bands.

These NDWI images were subtracted to achieve difference images. Pixel values of NDWI images range from -1 to +1 where positive values indicate water or higher soil moisture content. NDWI images do not fully remove the background soil reflectance effects. To overcome this limitation, we used three threshold values to delineate the overbank deposition extent. These NDWI-derived, threshold change values are 0.15, 0.3, and 0.45 for Sentinel images and 0.1, 0.2, and 0.3 for Planet images. The mapped areas of overbank deposition are shown in Figure 5.3.

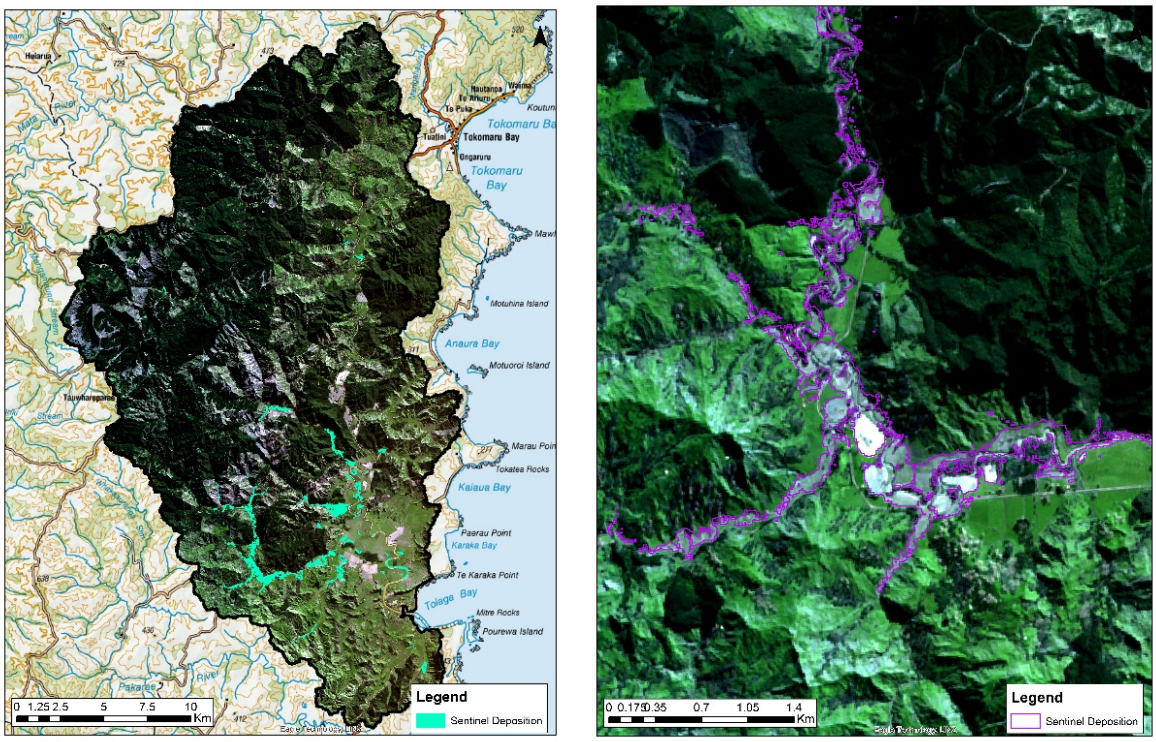

Figure 5.3 Mapped areas of overbank deposition from differencing of NDWI derived from Sentinel imagery.

5.2.3 Assessment of satellite differencing accuracy

5.2.3.1 Landslides

Satellite differencing (described above) was carried out using the before- and after-storm satellite images from Sentinel (10 m resolution), and Planet's Dove satellites (3 m resolution). Polygons were created to represent landslides triggered by the storm. There were significant differences in the basic landslide statistics derived from Sentinel and Planet differencing (Table 5.5). To assess the accuracy of the automated satellite differencing methodology to detect landslides we also manually mapped landslide source areas, deposits, and debris flow deposits using the SkySat imagery (0.8 m resolution). Aerial photography (0.3 m resolution) captured in 2017 and provided by GDC was used as the pre-storm baseline data.

Table 5.5 Comparison of automated landslide recognition results from differencing pre- and post-event Sentinel and Planet Dove satellite images.

Calculated landslide statistics	Sentinel	Planet Dove
Area covered (km^2)	560	452
No. of landslides	3931	11347
Average area of a landslide (m^2)	467.3	207.3
Total area of landslides (km^2)	1.8	2.4
Average landslide density (per km^2)	7.0	25.1

The automated processing was tested using three 1 km^2 windows in each of the three main land use classes (pasture, closed canopy (mature) forests, and recently harvested forests). The areas chosen were where imagery from all three satellite systems was available (Figure 5.4). Landslide statistics were calculated for each of the windows (pasture, mature forest, recently harvested forest), for each of the satellites systems (Sentinel, Planet Dove, Planet

SkySat). The results are presented in Table 5.6 and Figure 5.4 to Figure 5.7. In areas of mature forest and or recently harvested forest, landslides associated with infrastructure such as roads or landings were tagged.

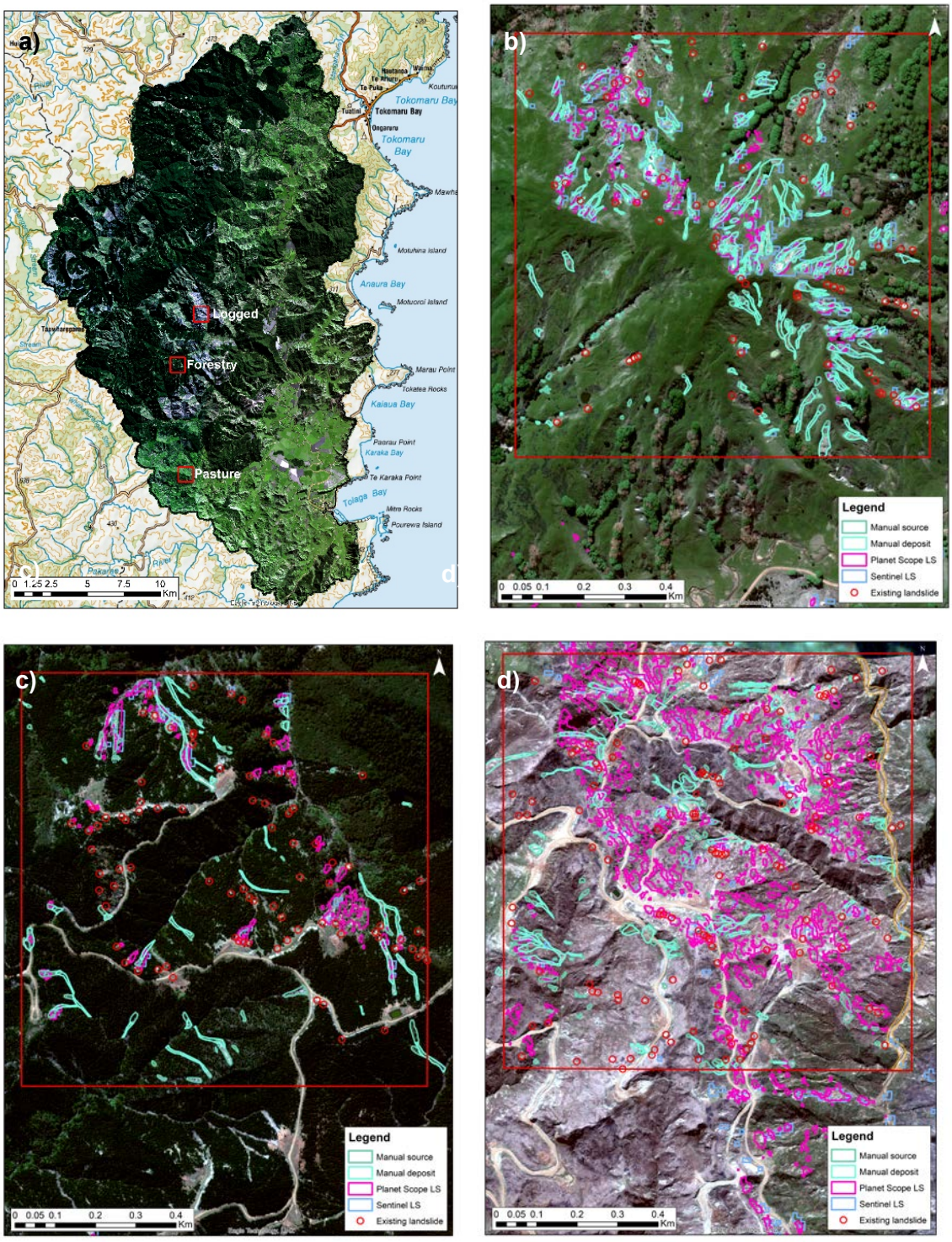

Figure 5.4 Landslide mapping in selected 1 km^2 areas using automated differencing for Sentinel and Planet Dove imagery and manual mapping of Planet SkySat images. a) Location of the 1km^2 land-use windows. Screenshots of the b) pasture c) mature forest and d) recently harvested areas, showing landslides mapped by all three methods. Existing landslides are also shown. The underlying imagery is post-event 0.8m SkySat imagery.

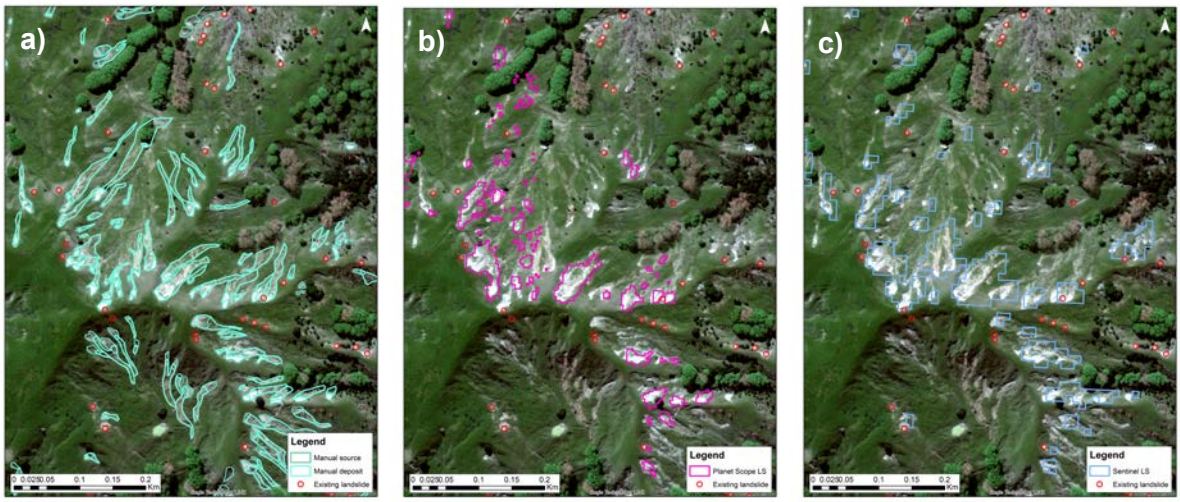

Figure 5.5 Comparison of landslides mapped on pasture a) manually on 0.8 m resolution SkySat imagery, to automatic classification of landslides from b) 3m resolution Planet and c) 10 m resolution Sentinel imagery.

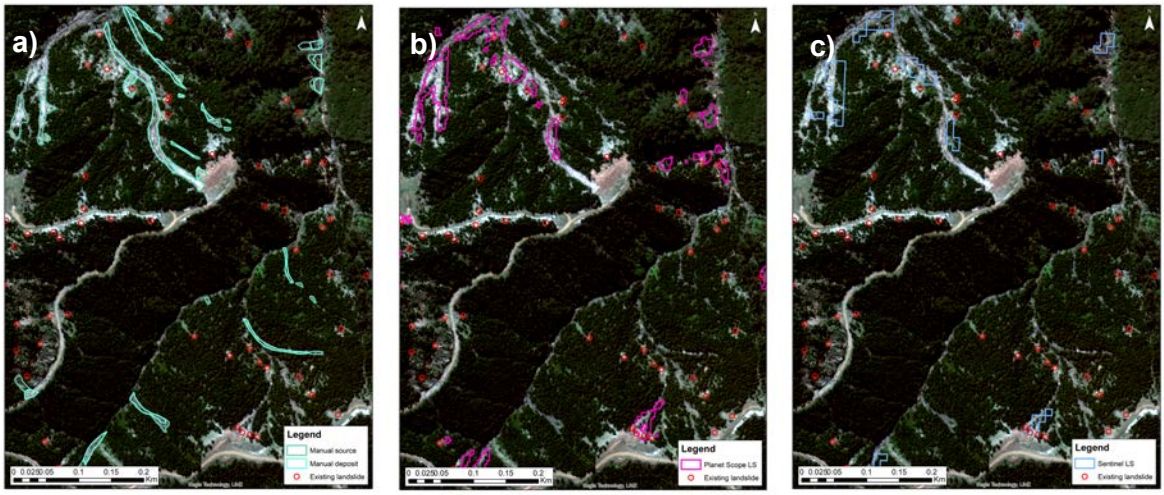

Figure 5.6 Comparison of landslides mapped on forestry a) manually on 0.8 m resolution SkySat imagery, to automatic classification of landslides from b) 3m resolution Planet and c) 10 m resolution Sentinel imagery.

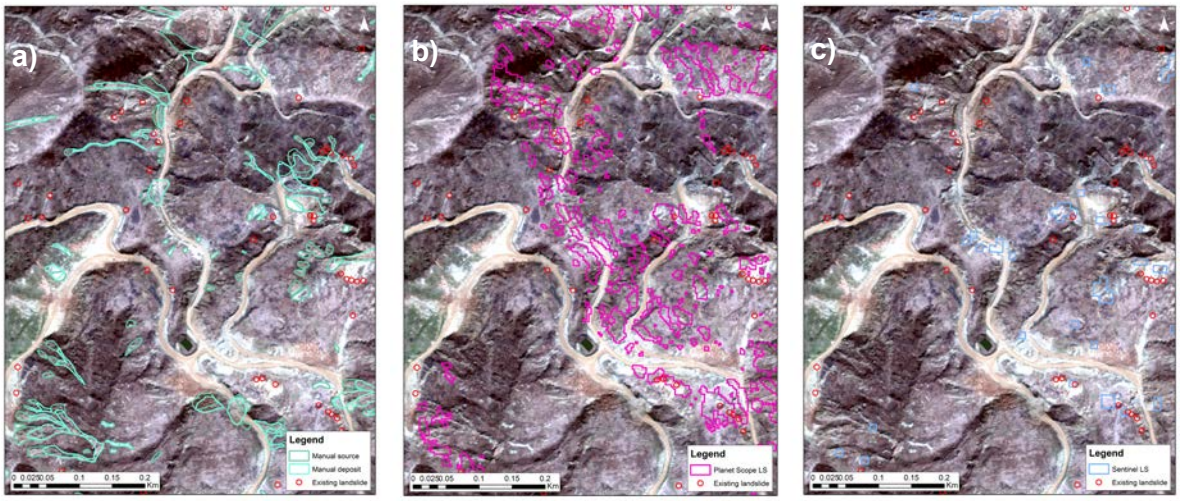

Figure 5.7 Comparison of landslides mapped on logged areas a) manually on 0.8 m resolution SkySat imagery, to automatic classification of landslides from b) 3 m resolution Planet imagery and c) 10 m resolution Sentinel imagery.

Table 5.6 Comparison of landslide statistics obtained from the different Satellite images (different resolution). For 1 km^2 detailed mapping areas. Figure in bold is significantly different from the manual mapping method at the 95 % confidence level. LS = landslide; Avg = average; Min = minimum; Max = maximum; SDV = standard deviation.

Land use	Landslide (LS) statistics	Sentinel (10 m)	Dove (3 m)	SkySat (0.8 m)
		Automated		Manual
Pasture	No. LS	70	164	217
	Total LS area	56,500	25,470	26,571
	Avg LS area	**807**	155	122
	Min LS area	100	9	11
	Max LS area	5,300	2,259	1,170
	SDV LS area	1,101	335	129
Mature Forest	No. LS	20	73	52
	Total LS area	8,900	18,621	12,574
	Avg LS area	445	255	242
	Min LS area	100	9	16
	Max LS area	2,100	2,529	1,000
	SDV LS area	491	476	238
Harvested	No. LS	71	526	162
	Total LS area	14,800	96,669	24,504
	Avg LS area	208	184	151
	Min LS area	100	9	15
	Max LS area	800	5,310	975
	SDV LS area	181	476	166

The only statically significant variation at the 95 % confidence level is the average source area of landslides measured by Sentinel on pasture (Figure 5.5) is significantly larger than the average source area of landslides measured manually. Other sample sizes were generally too small to determine if the mean areas are significantly different or not, given the variability. Results from Sentinel and Dove differencing were compared to the results for manual mapping and summarised below:

Dove:

- Underestimated number of landslides on pasture relative to manual mapping.
- Overestimated number in forest and logged areas relative to manual mapping.
- Good at estimating landslide areas, although small over-estimates of average landslide area for all land uses relative to manual mapping.
- Total landslide area accurate on pasture, overestimated in mature forest (50%) and harvested (400%) areas relative to manual mapping.

Sentinel:

- Underestimated number of landslides for all land uses (only recorded a third of all landslides) relative to manual mapping.
- Overestimated the average area of landslides on for all land uses relative to manual mapping.
- Total landslide area overestimated on pasture but underestimated in mature forest and harvested areas relative to manual mapping.

5.2.3.2 Deposition

A visual qualitative assessment was performed on the overbank deposition polygons generated by the Normalised Difference Water Index (NDWI) from Sentinel and Dove imagery. The NDWI derived from both sets of imagery provides a good representation of overbank sedimentation (Figure 5.8). NDWI derived from Sentinel imagery appears to be a more realistic representation of the areas of sedimentation because polygons covered the whole width of the floodplain that was inundated. NDWI derived from Dove imagery was very sensitive to small changes in soil moisture and provided an overcomplicated assessment of areas of overbank sedimentation. Areas of sediment deposition derived from Sentinel imagery were used in the sediment volume calculations.

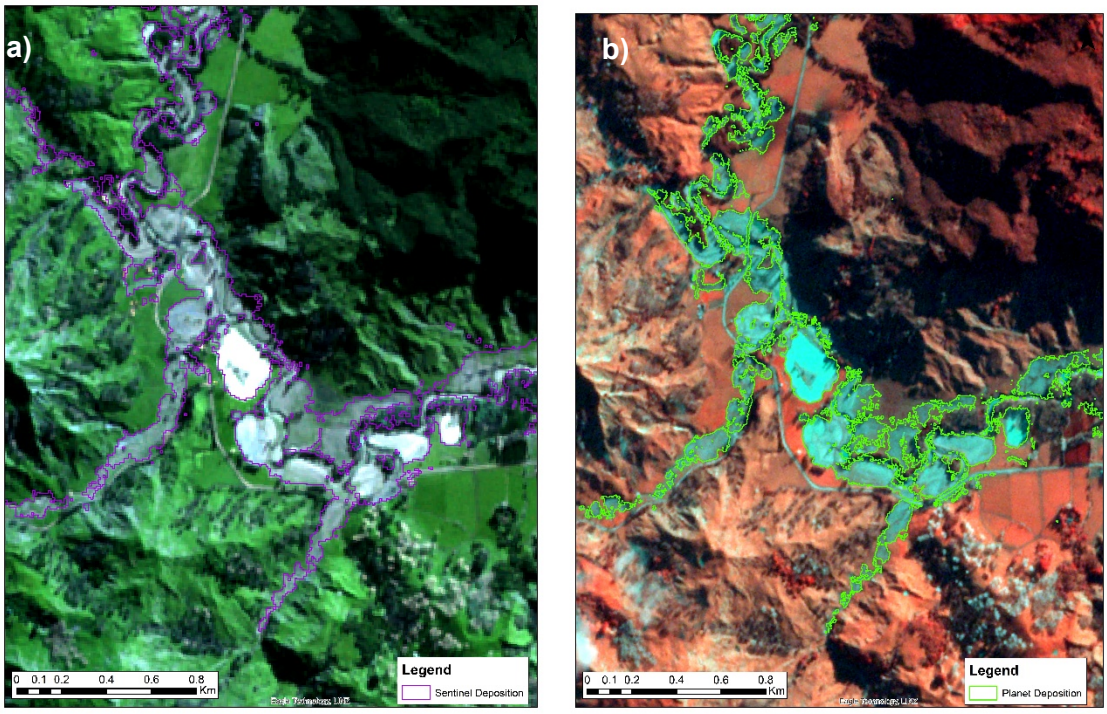

Figure 5.8 Comparison of areas of overbank deposition generated by the NDWI from a) Sentinel and b) Dove imagery.

6.0 ANALYSIS OF SEDIMENT LOSSES AND GAINS

6.1 Scaling from Landslide Area to Volumes

The areas of landslides triggered by the Queen's Birthday storm have been derived by satellite imagery differencing and manual mapping (for small 1 km^2 areas). To estimate the volume of sediment generated requires information on the depth of landslides perpendicular to the slope. No fieldwork was undertaken as part of this project to collect this data, so no field verification data was available on the depth of landslide source areas, depth of deposits or the depth of overbank sediments on the floodplains.

However, landslide source depth data was collected in the field from the adjacent Waipaoa catchment in 1996 after Cyclone Bola (in 1988). We have used this data to estimate landslide volumes in the Uawa River catchment after the June 2018 storms. In the Waipaoa, the dimensions of 95 landslides (length, width, depth), triggered by Cyclone Bola in March 1988 were measured (and area and volume were calculated) for different erosion terrains (Page et al 1999). From this data, area to volume scaling relationships (Figure 6.1) were developed for landslides on the different erosion terrains. These have been applied to landslides on the corresponding erosion terrains in the Uawa catchment (Section 3).

Landslide polygons generated from differencing Dove imagery were considered good enough to represent landslide areas triggered by the storm based on comparison with the detailed landslide mapping for pasture, forestry and logged areas (Table 5.6). Using the areas delineated by Dove satellite imagery differencing, a landslide size distribution was developed for each of the Uawa erosion terrains (Table 6.1). The number of landslides in each volume category was then multiplied by the volume (the minimum volume in each volume range) and summed to obtain a volume of sediment generated (in Dove area) for each erosion terrain. Because of differences identified between automated and manual mapping of landslides for different vegetation types, landslide areas were scaled (Section 5.2.3.1). The following section describes the scaling methodology. The volume of sediment generated in the Uawa catchment by landslides in the area captured by Dove satellite imagery was 3,784,350 m^3.

6.2 Scaling Automated Mapping to Manual Mapping

The polygons of landslides generated from differencing Dove imagery were chosen as the best representation of landslide numbers and areas (Section 5.2.3) for use in volume calculations. Dove imagery covers 82% of the Uawa catchment area. The remaining area (18%) is covered by 10 m resolution Sentinel imagery. Differencing of Sentinel imagery, in areas not covered by the Dove imagery, identified 845 landslides. However, the detailed 1 km^2 landslide manual mapping shows the differencing of pre- and post-event Sentinel imagery underestimates the number of landslides on pasture and overestimates landslides in forestry and logged areas (Table 5.6), compared to manual mapping (See section 5.2.3).

Adjusting the Sentinel-derived and the Dove-derived automated mapping data to match the results from manual mapping was carried out in the following way. The number (and percentage) of landslides in each vegetation class was determined for both Dove and Sentinel imagery (Table 6.2). In our study only three vegetation classes are used, exotic forest (closed canopy or mature forest), areas of harvested forest (harvested 6 years ago or harvested in the last 3 years) and grasslands (or pasture). The other vegetation classes combined represent less than 10% of the total land cover and are not considered in our analysis (Manuka and/or Kanuka; Indigenous forest; Deciduous hardwoods; Cropland; Gorse/broom; Other). For the Sentinel data, only landslides outside the area covered by the Dove imagery are included. The

landslide data were scaled using scaling relationships developed from the data for pasture, closed canopy forest and recently logged areas in Section 5.2.3 (Table 5.6).

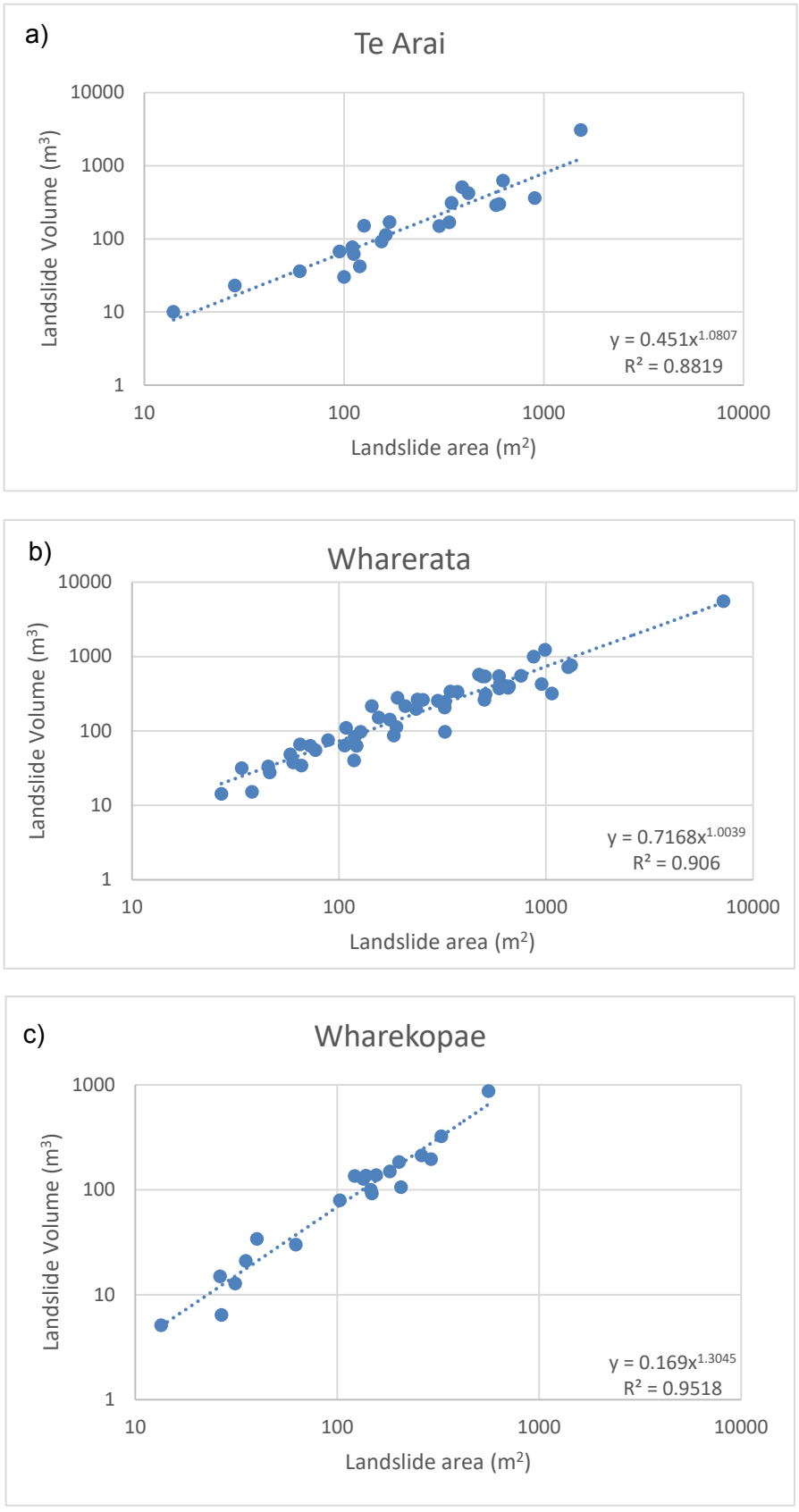

Figure 6.1 Area to volume scaling relationships for landslides in the Waipaoa catchment triggered by Cyclone Bola (1988) in the a) Te Arai, b) Wharerata and c) Wharekopae erosion terrains. Data from M. Page, Pers. Comm.

Table 6.1 Landslide size distribution for the three main erosion terrains in the Uawa catchment, derived from Dove landslide areas and area to volume scaling relationships for each erosion terrain.

Landslide size distribution							Volumes of sediment generated (m^3)		
LS Vol	Te Arai		Wharekopae		Wharerata		Te Arai	Wharekopae	Wharerata
m^3	no.	%	no.	%	no.	%			
0-1	0	0.0	0	0.0	0	0.0	0	0	0
1-10	2052	28.7	148	41.7	1005	27.4	20520	1480	10050
10-100	3390	47.4	133	37.5	1710	46.6	339000	13300	171000
100-500	1286	18.0	58	16.3	666	18.2	643000	29000	333000
500-1000	249	3.5	4	1.1	146	4.0	249000	4000	146000
1000-5000	168	2.3	12	3.4	131	3.6	840000	60000	655000
5000-10000	11	0.2	0	0.0	10	0.3	110000	0	100000
10000-20000	2	0.0	0	0.0	1	0.0	40000	0	20000
20000-50000	0	0.0	0	0.0	0	0.0	0	0	0
Total	**7158**	**100**	**355**	**100**	**3668**	**100**	**2241520**	**107780**	**1435050**
Total volume sediment generated (m^3)									**3,784,350**

For the Dove imagery the number of landslides on pasture was increased (24%) and for mature forest and harvested areas the number of landslides was decreased (by 40% and 325% respectively). For the Sentinel imagery the number of landslides was increased for all three vegetation classes, pasture (68%), mature forest (62%) and harvested areas (56%). After scaling to manual mapping was applied, the calculated number of landslides triggered by the Queen's Birthday storm in the Uawa catchment was 6677 (Table 6.3).

A landslide size distribution was calculated for each erosion terrain for Sentinel landslides outside the Dove area (n=1299; Table 6.3). This size distribution was used to derive the total volume of sediment generated by the Sentinel landslides. The volume of sediment derived was 413,220 m^3 (Table 6.4). This volume was added to the volume derived for the Dove area (3,784,350 m^3) to derive a total sediment volume generated for the Queen's Birthday storm of approximately 4,200,000 m^3.

6.3 Sediment Delivery

Areas of change identified by the satellite imagery differencing were categorised into landslide (source area plus deposit) and alluvial deposition. It was not possible using automated processing techniques on the satellite imagery to differentiate between landslide source area and landslide deposit due to the resolution of data capture.

A portion of the sediment mobilized by most landslides is redeposited before reaching a channel. Sediment delivery ratios for each of the erosion terrains in the Waipaoa catchment were calculated by Reid and Page (2002) who estimated sediment delivery for landslides generated by Cyclone Bola from aerial photographs. They found that for a representative Te Arai sub-catchment, 35% of the debris tails did not reach a watercourse; 40% of the debris tails travelled down a hillslope before depositing some sediment in a watercourse; and 25% of the landslides entered a watercourse and delivered all sediment. The differences between erosion terrains were found to be minimal and a sediment delivery ratio of 0.5 was assumed for landslides on all land systems in the Waipaoa catchment (Reid and Page 2002). The

sediment delivery ratio of 0.5 was based on Cyclone Bola rainfall of about 600 mm in the Waipaoa catchment and represents an extreme event (return period 100+ years, Page et al. 1999). Rainfall in the June 2018 storms was around 240 mm in the Uawa catchment (return period around 25 years for 12-hour event) so it is likely that the ephemeral stream network would not have extended as far upstream (into zero and 1st order channels). Therefore, the SDR may have been lower in the June 2018 event and the SDR of 0.5 represents a maximum estimate (see Page et al. 1999).

Table 6.2 Landslide statistics (number, percentage and landslide density) for the June 2018 rainstorms in the Uawa catchment for each vegetation class. The coverage of the catchment is complete with 82% of the area covered by Dove imagery (by preference) and the remaining area (18%) covered by Sentinel imagery.

Vegetation Class (LCDBv4.1)	Area	Dove Landslides			Sentinel Landslides		
	km^2	No.	%	LS/km^2	No.	%	LS/km^2
Exotic Forest	111.9	3544	31.5	31.7	23	2.7	0.2
Forest - harvested (3-6 yrs)	25.0	892	7.9	35.7	27	3.2	1.1
Forest - recently harvested (<3yrs)	90.6	4458	39.6	49.2	501	59.3	5.5
Grassland/Pasture	174.9	1701	15.1	9.7	212	25.1	1.2
Manuka and/or Kanuka	88.6	423	3.8	4.8	29	3.4	0.3
Indigenous forest	32.7	204	1.8	6.2	13	1.5	0.4
Deciduous Hardwoods	7.9	3	0.0	0.4	10	1.2	1.3
Cropland	18.8	13	0.1	0.7	0	0.0	0.0
Gorse/Broom	0.7	0	0.0	0.0	4	0.5	5.7
Other (e.g. landslide scars, gravel)	0.7	14	0.1	20.0	26	3.1	37.1
Total	560.1	11252	100		845	100.0	

Table 6.3 Numbers of landslides from Dove and Sentinel automated differencing results (Table 6.2) scaled to reflect the results from manual mapping (Table 5.6). The landslide density for each vegetation class is shown. In our study scaling relationships for only three vegetation classes were available, exotic forest (closed canopy or mature forest), areas of harvested forest (harvested 3 to 6 years ago or harvested in the last 3 years) and grasslands (or pasture). The other vegetation classes combined represent less than 10% of the total land cover and were not scaled in our analysis (Manuka and/or Kanuka; Indigenous forest; Deciduous hardwoods; Cropland; Gorse/broom; Other).

Vegetation Class (LCDBv4.1)	Area	Planet	Sentinel	TOTAL (scaled to manual)		
	km^2	No.	No.	no.	%	LS/km^2
Exotic Forest	111.9	2127	37	2164	32.4	19.3
Forest - Harvested (6 yrs)	25.0	397	42	439	6.6	17.5
Forest - Recently logged (3 yrs)	90.6	1981	782	2763	41.4	30.5
Grassland/Pasture	174.9	217	356	573	8.6	3.3
Manuka and/or Kanuka	88.6	423	29	452	6.8	5.1
Indigenous forest	32.7	204	13	217	3.2	6.6
Deciduous Hardwoods	7.9	3	10	13	0.2	1.6
Cropland	18.8	13	0	13	0.2	0.7
Gorse/Broom	0.7	0	4	4	0.1	5.7
Other (existing LS, gravel, freshwater veg)	0.7	14	26	40	0.6	57.1
Total	**560.1**	**5378**	**1299**	**6677**	**Avg**	**11.9**

Table 6.4 Automated differencing of Sentinel imagery scaled to manual mapping to produce numbers relative to the size distribution and volumes of sediment per erosion terrain.

Volume		Numbers of landslides (n=845)			All erosion terrains		Sentinel scaled (n=1299)			Sentinel Volumes		
m^3		Te Arai	Wharekopae	Wharerata	No. LS	Volume	Te Arai	Wharekopae	Wharerata	Te Arai	Wharekopae	Wharerata
1		0	0	0	0	0	0	0	0			
10		212	12	18	242	2422	330	19	27	3299	188	274
100		351	11	30	392	40019	545	17	47	54511	1686	4662
500		133	5	12	150	75906	207	7	18	103394	3676	9078
1000		26	0	3	29	29394	40	1	4	40039	507	3980
5000		17	1	2	20	99162	27	2	4	135071	7606	17857
10000		1	0	0	1	12985	2	0	0	17688	0	2726
20000		0	0	0	0	4722.	0	0	0	6432	0	545
50000		0	0	0	0	0.	0	0	0	0	0	0.
%		88	3	8								
Total		741	29	65	845	264611	1151	45	100	360434	13662	39124
Volume sediment area outside imagery												413,220

A sediment delivery ratio of 0.5 was applied to landslides in the Uawa. Based on this ratio, the volume of sediment delivered to the Uawa River by landslides triggered by the June 2018 rainstorms was approximately 2,100,000 m^3. Using a bulk density of 1.25 kg/dm^3 for typical soils in the Waipaoa catchment (equivalent to Uawa soils) (Reid and Page 2002), this is approximately 2,625,000 tonnes of sediment.

6.4 Sediment Deposition

Areas of sediment deposition were identified by the satellite differencing as described in Section 5.2.3. No information on the depth of material deposited on the floodplain was available, so no estimates of sediment volumes could be made. The second storm event was a moderate event in the Uawa catchment and it is assumed no overbank sedimentation occurred (Cave pers. comm.). The total areas of overbank sedimentation for different sub-catchments in the Uawa River are presented in Table 6.5. The area of overbank sedimentation derived from Sentinel was 4.26 km^2, or 426 ha.

Table 6.5 Areas of deposition in the Queen's Birthday Storm as recorded by Sentinel and Dove satellites.

Sub-catchment	Area m^2	
	Sentinel	**Planet**
Hikuwai	114500	219447
Kaitawa	84400	-
Mangaheia	2308500	1437214
Mangarakai	2500	-
mangatokerau	387500	95463
Uawa	1337100	1144764
Waiau	16700	-
Whangara	6300	-
Total	4257500	2896888
	4.26 km^2	2.90 km^2

Once in the channel system, some portion of the mobilized sediment is deposited on downstream floodplains, decreasing the overall delivery ratio to sites farther downstream. Reid and Page (2002) determined that approximately 5% to 10% of the sediment generated by landslides in the Waipaoa catchment was expected to be lost to overbank deposition.

If 2,100,000 m^3 of material was delivered to the river by landslides in the storm, then about 105,000 to 210,000 m^3 of material could be expected to be deposited on the floodplain. Using the area of deposition from Sentinel differencing (4.26 km^2), the average depth of sediment would be roughly 25 to 50 mm, which is considered reasonable as there was not widespread reports of fences being partially buried by sediment on the floodplains.

7.0 LANDSLIDE SEVERITY AND DISTRIBUTION

There were approximately 6677 landslides triggered by the Queen's Birthday storm in the Uawa catchment (Table 6.2). They occurred over an area of about 414.5 km^2, in the western and northern parts of the catchment (Figure 7.1). The average landslide density was 16.1 landslide/km^2. The total area affected by landslides was approximately 2.4 km^2 (from Dove differencing; not scaled)

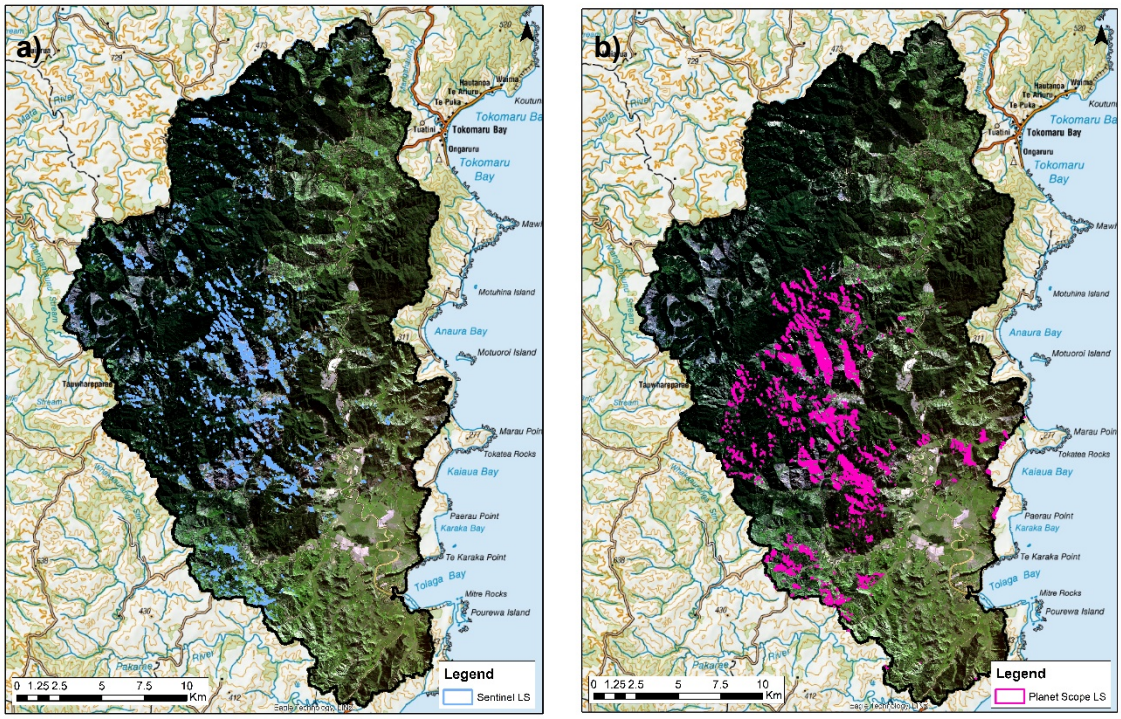

Figure 7.1 Mapped landslide distribution from the Queen's Birthday storm in the Uawa catchment using automatic extraction of landslides from a) Sentinel and b) Dove imagery differencing.

7.1 Controls on Landslide Distribution

7.1.1 Rainfall

The highest landslide densities in the Uawa catchment generally occurred in areas with the highest rainfall (Figure 7.2). Landslide densities increased logarithmically with total storm rainfall up to 100 mm (equivalent to a rainfall intensity of 12.5 mm/hr over eight hours) and then decreased slightly. The reasons for this are unclear but may relate to the three-way relationship between rainfall, vegetation and slope which has not been investigated in this work.

Most landslides occurred on areas that had been logged in the last six years rather than where the highest rain fell. This indicates land-use practices may be as strong (or stronger) as a determinant of landslide occurrence than total rainfall.

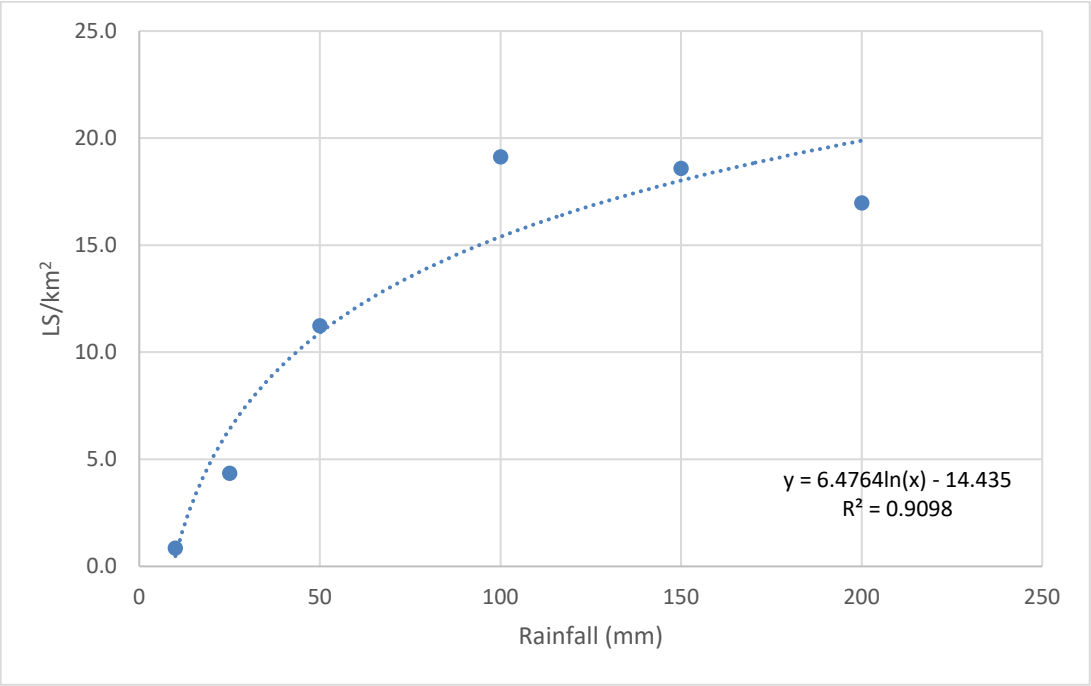

Figure 7.2 Relationship between rainfall (8hr) and landslide density.

7.1.2 Geology/Erosion terrain

There were similar landslide densities on both Te Arai (8.1 landslides/km^2) and Wharerata (9.2 landslides/km^2) erosion terrains (Table 7.1). This is not surprising because both erosion terrains are underlain by poorly consolidated Tertiary aged sedimentary rocks. Hillslopes underlain by the Wharekopae erosion terrain showed the lowest landslide density. These slopes are generally less steep and are mantled with tephra making them less susceptible to landslides.

Table 7.1 Numbers of landslides and density using the numbers of landslides generated from Sentinel imagery differencing. The numbers from Sentinel differencing were used here because Sentinel imagery covers the whole catchment, however, these numbers are a minimum because differencing of Sentinel imagery was shown to underestimate landslide numbers on all vegetation types.

Erosion terrain	Area (km^2)	% catchment	No. LS	LS density (LS/km^2)
Te Arai	329.7	58.9	2654	8.1
Wharerata	115.6	20.6	1065	9.2
Wharekopae	37.3	6.7	114	3.1
Other	77.4	13.8	0	0
	560.0	100	3833	

7.1.3 Slope

There is a direct correlation between slope and landslide density. Landslide density increased as a function of slope, so there were more landslides on steeper hillslopes (Figure 7.3).

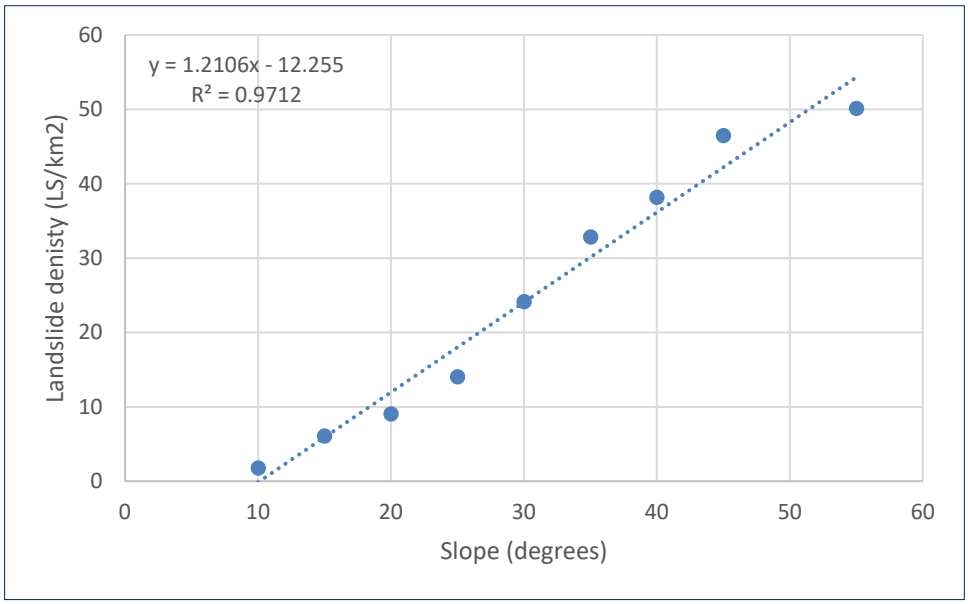

Figure 7.3 Relationship between slope and landslide density.

7.1.4 Aspect

The slope aspect where landslides occurred generally reflects the distribution of slope aspect within the catchment (Figure 7.4). This shows slope aspect of the hillslopes had a strong influence on the location of landslides in the June 2018 rainstorms and the distribution of landslides was not influenced by the direction of the prevailing winds during the storm (from the north-west).

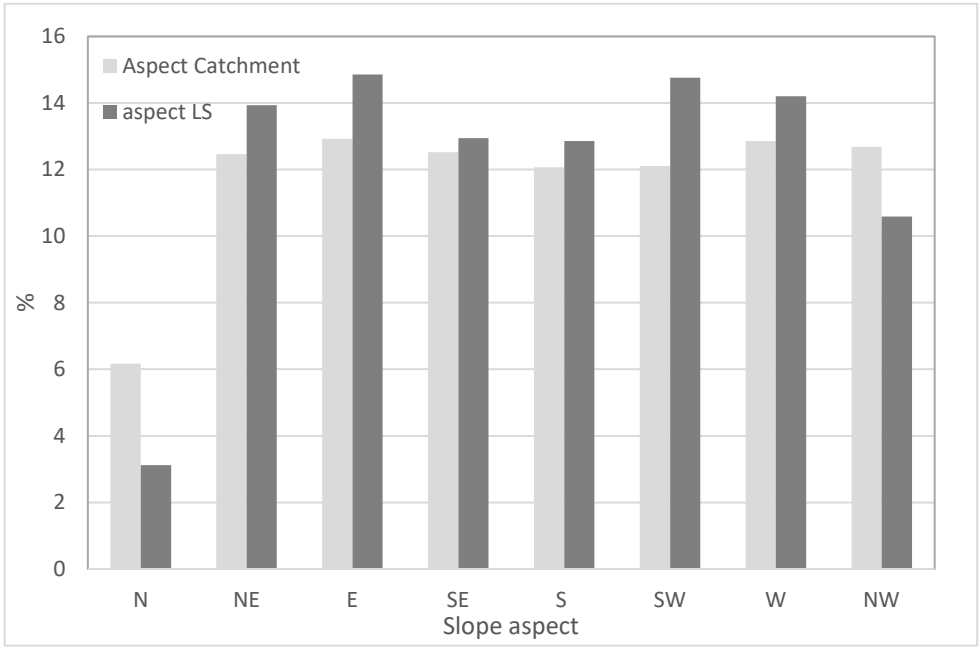

Figure 7.4 Slope aspect of hillslopes that landslides were triggered on compared to the aspect of hillslopes in the Uawa catchment

7.1.5 Vegetation

The highest landslide densities (30.5 landslides/km^2) were recorded on slopes where the forests had been harvested in the last 3 years (Table 7.2). Many of these areas were being harvested when the storm occurred. Landslide densities recorded on hillslopes covered in mature exotic forest plantations (19.3 landslides/km^2) or forest that had been harvested 3-6 years ago (17.5 landslides/km^2) and replanted were similar. The landslide density on hillslopes in pasture was relatively low (3.3 landslides/km^2) compared to areas in exotic forest. This may be due to slopes that are most vulnerable to erosion having been planted in forests. At the time of the storm some 20% of the catchment had been harvested in the previous six years. This area (116 km^2) was particularly vulnerable to erosion and 47% of the landslides that occurred had source areas on hillslopes that had been logged in the last six years.

Table 7.2 Landslide numbers (scaled to manual mapping) and densities for the main vegetation classes in the Uawa catchment.

Vegetation Class	Area (km^2)	% area	no. LS	%	LS/km^2
Exotic Forest	111.9	20.0	2163	32.4	19.3
Forest - Harvested (6 yrs)	25.0	4.5	438	6.6	17.5
Forest - Recently logged (3yrs)	90.6	16.2	2762	41.4	30.5
Grassland/Pasture	174.9	31.2	573	8.6	3.3
Manuka and/or Kanuka	88.6	15.8	452	6.8	5.1
Indigenous forest	32.7	5.8	217	3.2	6.6
Deciduous Hardwoods	7.9	1.4	13	0.2	1.6
Cropland	18.8	3.4	13	0.2	0.7
Gorse/Broom	0.7	0.1	4	0.1	5.7
Other (existing LS, gravel, freshwater veg)	0.7	1.7	40	0.6	57.1
Total	560.1	100.0	6677	100.0	

In the 1 km^2 detailed mapping windows for harvested areas 46% of landslides were associated with logging/forestry infrastructure such as roads and landings. In closed canopy (mature) forest, 31 % of landslides were associated with forest infrastructure.

An anomalously high landslide density (57.1 landslides/km^2) was recorded for areas mapped as ‘Other’ in LCDB4.1. This category includes existing landslide scars as well as gravel and freshwater vegetation associated with rivers. These landslides may be from river bank erosion, or reactivation or enlargement of existing landslides. This land-use category only occupies 1.7% of the total catchment area.

8.0 DISCUSSION

8.1 Landslides Triggered by the Queen's Birthday Storm

Extensive landsliding was triggered in the Uawa catchment by the Queen's Birthday storm on 3rd and 4th June 2018. The predominant landslide types were shallow (~1m depth) translational soil slides, debris slides and debris flows, on newly harvested forestry land. Landslides triggered by the storm also occurred on hillslopes with both exotic forest and indigenous forest. Debris floods and debris flows occurred in many of the river and stream channels downstream of the landslides and transported woody debris from areas of recently harvested forest in the headwater catchments, downstream to the floodplain and coast at Tolaga Bay.

The sediment volume produced by these landslides was estimated by satellite imagery differencing to be about 4.2 M m^3, and about half of this (2.1 M m^3) or 2.6 M tonnes was delivered to the Uawa River system. This compares to a sediment volume produced during Cyclone Bola in 1988, the largest storm on record for the Uawa catchment, of ~68 M m^3 (Marden et al 1991). There are two reasons for the large difference in sediment generation between the two storms. Firstly, Cyclone Bola delivered 900 mm of precipitation over 5 days, so was a much more extreme and prolonged storm event. Secondly, in 1988 when Cyclone Bola hit, 26% (or 12,500 ha) of steep hill country in the Uawa catchment were planted in exotic forest, however, 98% of these forests were less than 8-years old (Marden et al 1991). For New Zealand plantation forests, there is a window of between 4-8 years from clear-felling until canopy closure of the new tree crop rotation, where plantation sites are more susceptible to erosion (Marden et al 1991; Phillips et al 1990; Bloomberg et al 2011). Although many of the steep erosion-prone hillslopes were planted in forestry, their young age meant they had limited effectiveness at preventing erosion. Given that plantation forests are known to decrease landslide rates on the East Coast by approximately ten times (Phillips et al 1990), this would account for much of the difference in sediment generation between 1988 and 2018 storms.

Landslide densities were highest in areas of exotic plantation forest that had been logged within the last 3 years. Landslide densities were also relatively high on areas that had been logged 3-6 years ago and in areas of established exotic forest. In the recently logged areas, about half (46%) of the landslides were associated with forestry infrastructure such as logging roads and haul sites or landings. The percentage of landslides that were associated with forestry infrastructure on slopes in established exotic forest was also relatively high at around 30% (see Figure 4.5). Phillips et al (2012) found plantation forests located on steeplands were more prone to shallow landsliding in the 4-8 years following harvest than at any other time in the plantation forestry cycle.

There were relatively low landslide densities on pasture (3.3 landslides/km^2), compared to landslide densities on slopes with exotic forest (19.3 landslides/km^2) and indigenous forest (6.6 landslides/km^2). This is most likely because of the targeting of afforestation to steeper slopes underlain by erosion-prone rock types - the area's slopes most susceptible to erosion. The average slope of hillslopes in pasture ranged from 16.2 to 20.2 degrees, compared to the average slope of hillslopes in plantation forestry which ranged from 27.5 to 35.4 degrees.

In addition, higher landslide densities were observed in areas that received the highest rainfall. The slope was also an important control on the landslide distribution, with the number and density of landslides increasing on steeper slopes. Geology and erosion terrain was also important, although most of the catchment is composed of highly erodible lithologies so the differences between the rock types and erosion terrains was minimal.

8.2 Limitations of Satellite Imagery Differencing to Detect Landslides

To assess the extent of damage associated with landslides in a storm event, and to estimate a sediment volume produced by the landslides usually requires a combination of ground-based assessments of landslide size and type in combination with aerial photo interpretation and mapping, both of which are very time consuming and have very high costs associated with them. An issue with this approach is that it is not always possible to establish if slope failures resulted from a specific event or from multiple events over a number of years, depending on the availability of aerial pre- and post-event aerial photography. GDC was interested in whether differencing analysis pre- and post-event satellite imagery could provide a rapid and cost-effective tool for providing a credible quantification of the environmental impact of landsliding resulting from severe storms. We compared the results of satellite image differencing from two different resolution satellites (10 m Sentinel and 3 m Planet Dove) to what we would achieve with manual landslide mapping using sub-metre resolution satellite imagery (Planet SkySat 0.8 m).

There were several issues identified with differencing from both Sentinel and Planet Dove imagery. The issues were generally associated with the resolution of the imagery, sensor sensitivity, and areas of shadows. Registration issues were also important.

Differencing of Sentinel imagery produced a quarter of the number of landslides derived from Planet Dove differencing. Although the sensor on Sentinel can pick up subtle changes in reflectance, the resolution of the imagery (10 m) meant that several landslides were often combined into a single polygon, and we were not able to differentiate between landslide source and deposit. Often the debris tails were too small to be detected. Most rainfall-induced landslides on highly erodible land on the East Coast of the North Island are small (average area was ~150 m^2), shallow soil slides and flows so appear as a single pixel (100 m^2) in the difference image. The small distances between landslides also meant that it was not possible to differentiate between individual landslides from the Sentinel imagery. In addition, many mis-classifications of roads, skid sites and landings and ploughed areas were identified in the analysis.

By comparison, differencing of the 3 m spatial resolution of Planet Dove imagery was better at accurately detecting the number and areas of landslides on both pasture and forestry. Detecting landslides in logged areas, and areas of pre-existing landslides, however, was less accurate using the Dove imagery. In some instance multiple polygons were produced for one landslide, where the sensor differentiated between different reflectance's across a landslide (due to small changes in vegetation, shadowing, soil moisture). Dove imagery differencing was also not able to differentiate between landslide source area and deposit.

Detecting landslides in logged areas from both imagery sources was inaccurate because the spectral difference between landslides and disturbed ground in newly logged areas is minimal. There were also issues with detecting landslides in areas of shadow from both sets of imagery.

Landslide detection from differencing of satellite imagery is quicker and cheaper than traditional landslide mapping methods, however, the errors and misclassifications can be significant. To achieve landslide distributions and statistics that accurately portray the landslides on the ground systematic review and editing of landslide polygons is required. As a minimum, a comparison of landslide distributions obtained by satellite images should be checked against what would be produced by manual mapping using high resolution satellite imagery or aerial photography, so that appropriate scaling relationships can be developed for different vegetation types.

9.0 CONCLUSIONS

- Extensive landsliding was triggered in the Uawa catchment by the Queen's Birthday storm on June 3rd and 4th, 2018. The predominant landslide types triggered were shallow (~1m depth) translational soil slides, debris slides and debris flows.
- A second storm hit the Gisborne region on June 11th and 12th. This storm caused some additional localised landslides in the Uawa catchment and some reworking and remobilisation of landslides triggered by the earlier, Queen's birthday storm. Closed canopy (mature) forests were generally not affected. It was assumed that the storm with the greatest rainfall (June 3-4) triggered the landslides.
- Landslides were mapped using satellite imagery differencing of 10 m resolution Sentinel imagery, and 3 m resolution Planet Dove imagery. The results of this automated mapping were compared to the results from manual landslide mapping using 0.8 m resolution Planet SkySat imagery.
- Approximately 6680 landslides triggered by the 3rd – 4th June Queen's Birthday storm have been mapped in the Uawa catchment, Tologa Bay. The average landslide density was 16.1 landslide/km^2 and the total area affected by landslides was approximately 2.4 km^2.
- The estimated volume of sediment produced by landslides in the storm event was 4,200,000 m^3, of this approximately half of this (2.1 M m^3) or 2,625,000 tonnes was delivered to the Uawa River system.
- An area of 426 ha was affected by overbank sedimentation during the flooding associated with the storm event. The estimated average depth of overbank sediment was 25 to 50 mm, giving a total of volume of roughly 100,000 to 200,000 m^3.
- Landslide densities were highest in areas of exotic plantation forest that had been logged within the last 3 years. Landslide densities were also relatively high on areas that had been logged 3-6 years ago and in areas of established exotic forest. Landslide densities were much lower on areas of pasture.
- In the recently logged areas, about half (46%) of the landslides were associated with forestry infrastructure such as logging roads and haul sites or landings. The percentage of landslides that were associated with forestry infrastructure on slopes in established exotic forest was also relatively high (30%).
- Although differencing of satellite imagery is quicker and cheaper than traditional landslide mapping methods, the errors and misclassifications are potentially significant, and to achieve a landslide distribution and statistics that accurately portrays the landslides on the ground requires considerable checking and editing of landslide polygons. At the minimum, a comparison of landslide distributions obtained by satellite images should be checked against what would be produced by manual mapping using high resolution satellite imagery or aerial photography, so that appropriate scaling relationships can be developed for different vegetation types.

10.0 ACKNOWLEDGEMENTS

Funding for this study was provided by Envirolink and through GeoNet. Gisborne District Council provided the following assistance: analysis and shapefiles of rainfall data, shapefiles of recent logging areas. The Council also provided pre-storm orthorectified aerial photographs. Mike Page and Jon Carey (GNS Science) reviewed the report.

11.0 REFERENCES

Bloomberg M, Davies T, Visser R, Morgenroth J. 2011. Erosion susceptibility classification and analysis of erosion risks for plantation forestry. Christchurch (NZ): University of Canterbury, NZ School of Forestry. Prepared for the Ministry for the Environment.

Cave MP. 2018a. Analysis of rainfall for the storm events of 3rd- 4th June. East Coast Tairawhiti. Unpublished report. 36 p. Located at: Gisborne District Council, Gisborne, NZ.

Cave MP. 2018b. Analysis of rainfall for the storm events of 11th-12th June. East Coast Tairawhiti. Unpublished report. 33 p. Located at: Gisborne District Council, Gisborne, NZ.

Cave MP. 2019. Analysis of landslide events in the Wakaroa and Makiri Forests, and adjacent areas. Unpublished report. 23 p. Located at: Gisborne District Council, Gisborne, NZ.

Hungr O, Leroueil S, Picarelli L. 2014. The Varnes classification of landslide types, an update. *Landslides*. 11(2):167–194. doi:10.1007/s10346-013-0436-y.

Dymond JR, Betts HD, Schierlitz CS. 2010. An erosion model for evaluating regional land-use scenarios. *Environmental Modelling & Software*. 25(3):289–298. doi:10.1016/j.envsoft.2009.09.011.

Lynn IH, Manderson AK, Page MJ, Harmsworth GR, Eyles GO, Douglas GB, Mackay AD, Newsome PJF. 2009. Land use capability survey handbook: a New Zealand handbook for the classification of land. 3rd ed. Hamilton (NZ): AgResearch Limited. 163 p.

Marden M, Phillips C, Rowan D. c1992. Declining soil loss with increasing age of plantation forests in the Uawa Catchment, East Coast Region, North Island, New Zealand. In: Henriques P, editor. *Sustainable land management: the proceedings of the International Conference on Sustainable Land Management*. 1991 Nov 17-23; Napier, New Zealand. Napier (NZ): Organising Committee. p. 358–361.

Marden M, Rowan D, Phillips C. 1995. Impact of cyclone-induced landsliding on plantation forests and farmland in the East Coast Region of New Zealand: a lesson in risk management. In: Sassa K, editor. *Proceedings of the XX IUFRO World Congress Technical session on natural disasters in mountainous areas*. 1995 Aug 7-10; Tampere, Finland. Jvyäskylä (FI): Finnish IUFRO World Congress Organising Committee. p. 133–145.

Mazengarb C, Speden IG, compilers. 2000. Geology of the Raukumara area [map]. Lower Hutt (NZ): Institute of Geological & Nuclear Sciences Limited. 1 folded map + 60 p., scale 1:250,000. (Institute of Geological & Nuclear Sciences 1:250,000 geological map; 6).

Page MJ, Reid LM, Lynn IH. 1999. Sediment production from Cyclone Bola landslides, Waipaoa catchment. *Journal of Hydrology, New Zealand*. 38(2):289–308.

Phillips CJ, Marden M, Pearce A. 1990. Effectiveness of reforestation in prevention and control of landsliding during large cyclonic storms. In: *Proceedings of the International Union, Forest Research Organisations 19th World Congress*; 1990 Aug 5–11; Montreal, QC. Vienna (AT): IUFRO. p. 340–350.

www.gns.cri.nz

Principal Location

1 Fairway Drive
Avalon
PO Box 30368
Lower Hutt
New Zealand
T +64-4-570 1444
F +64-4-570 4600

Other Locations

Dunedin Research Centre
764 Cumberland Street
Private Bag 1930
Dunedin
New Zealand
T +64-3-477 4050
F +64-3-477 5232

Wairakei Research Centre
114 Karetoto Road
Wairakei
Private Bag 2000, Taupo
New Zealand
T +64-7-374 8211
F +64-7-374 8199

National Isotope Centre
30 Gracefield Road
PO Box 31312
Lower Hutt
New Zealand
T +64-4-570 1444
F +64-4-570 4657

Phillips C, Marden M, Basher L. 2012. Plantation forest harvesting and landscape response – what we know and what we need to know. *New Zealand Journal of Forestry*. 56(4):4–12.

Reid LM, Page MJ. 2003. Magnitude and frequency of landsliding in a large New Zealand catchment. *Geomorphology*. 49(1–2):71–88.